Electronic Supplementary Information

Distinct Modes of Si-H Binding to Rh in Complexes of a Phosphine-Diarylamido-Silane (SiNP) Pincer Ligand

A. Rain Talosig[a], Mario N. Cosio[b], Benjamin Morse[a], Vinh T. Nguyen[b], Alex J. Kosanovich[b], Christopher J. Pell[b], Chun Li[a], Nattamai Bhuvanesh[b], Jia Zhou[c], Anna S. Larsen[a]*, and Oleg. V. Ozerov[b]**

*Corresponding authors, ozerov@chem.tamu.edu; alarsen@ithaca.edu; jiazhou@hit.edu.cn

[a] *Department of Chemistry and Biochemistry, Ithaca College, Ithaca New York, 14850, USA*

[b] *Department of Chemistry, Texas A&M University, TAMU – 3255, College Station, TX 77842, USA.*

[c] *State Key Laboratory of Urban Water Resource and Environment, Harbin Institute of Technology, Harbin 150090, China*

Table of Contents

1. Graphical NMR Spectra of (SiNP)Rh Complexes

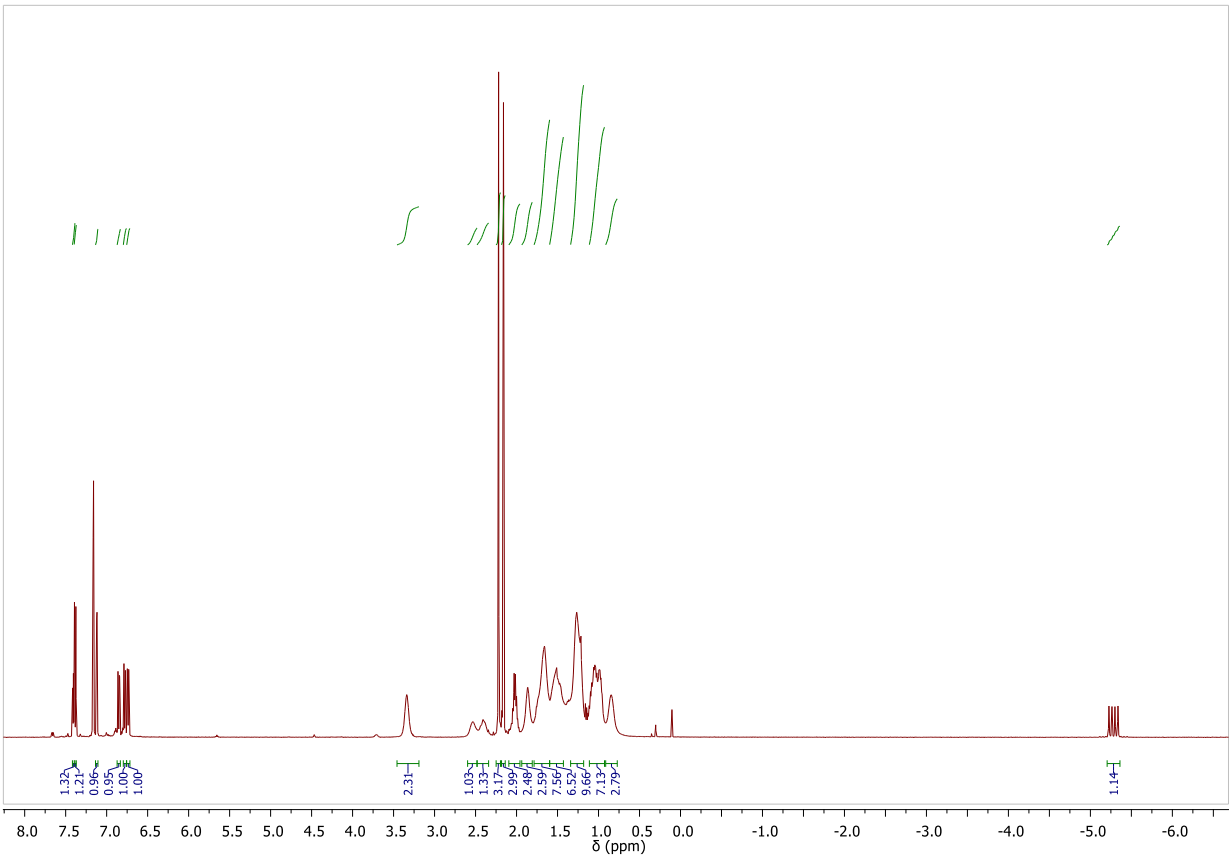

Figure S1. ^{1}H NMR (500 MHz, C_6D_6) spectrum of (SiNP)Rh(COE) (**5**). Sample contains small amount of residual silicone grease and hexamethyldisiloxane.

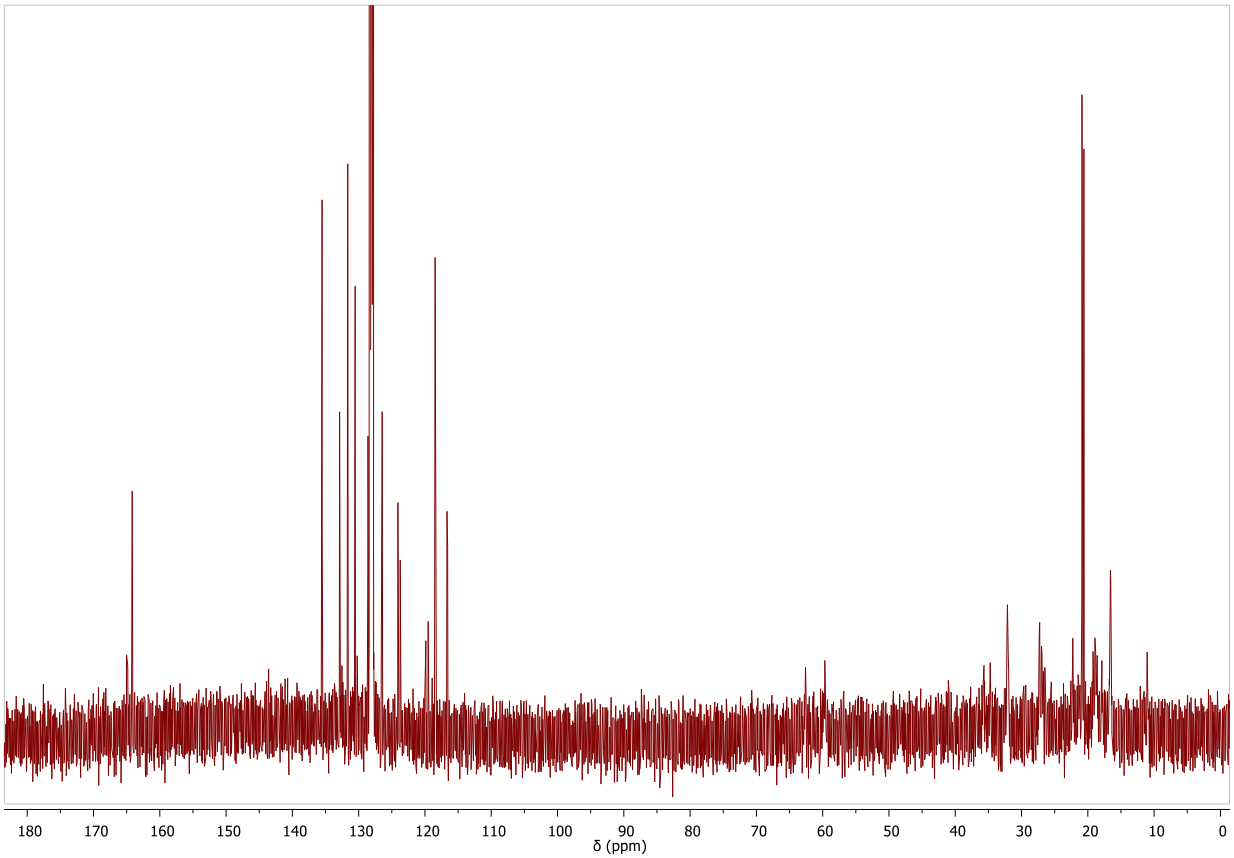

Figure S2. $^{13}C\{^{1}H\}$ NMR (128 MHz, C_6D_6) spectrum of (SiNP)Rh(COE) (**5**).

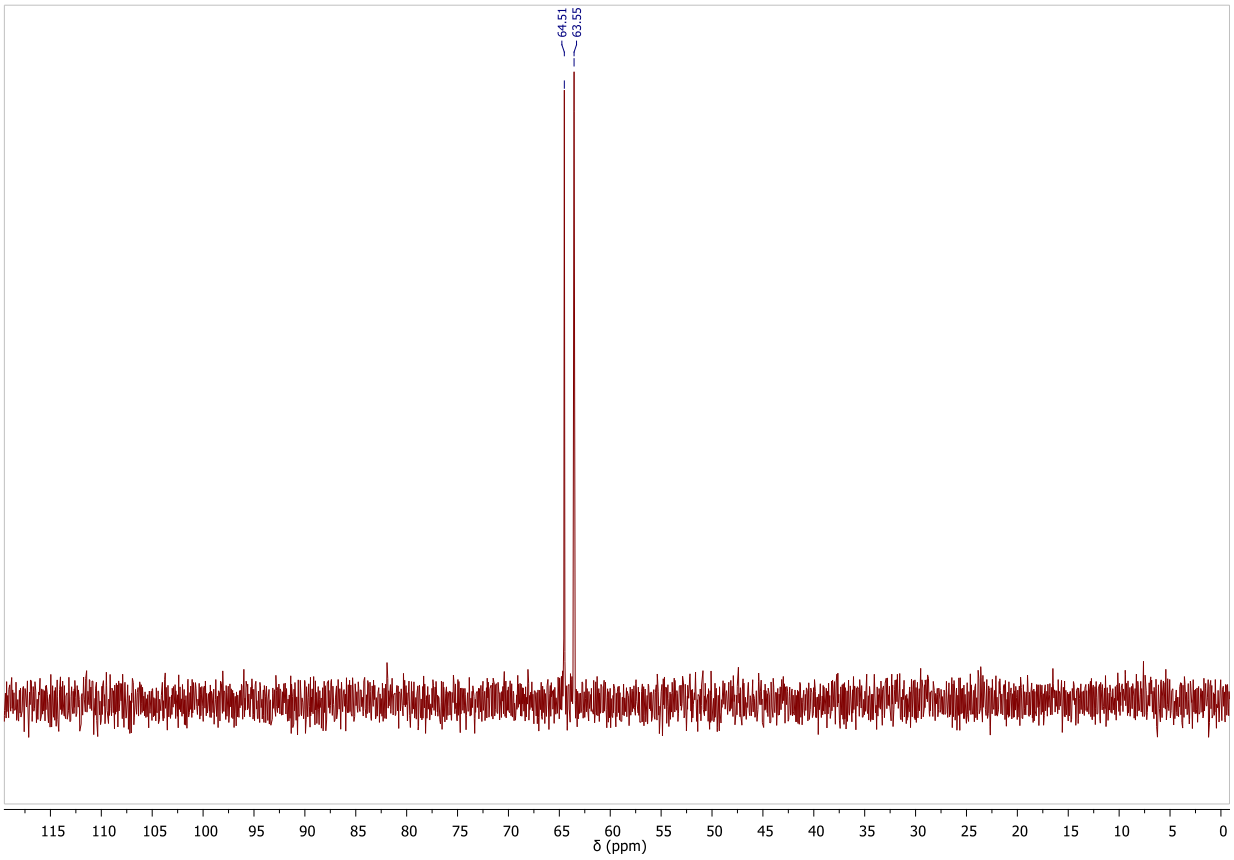

Figure S3. $^{31}P\{^{1}H\}$ NMR (202 MHz, C_6D_6) spectrum of (SiNP)Rh(COE) (**5**).

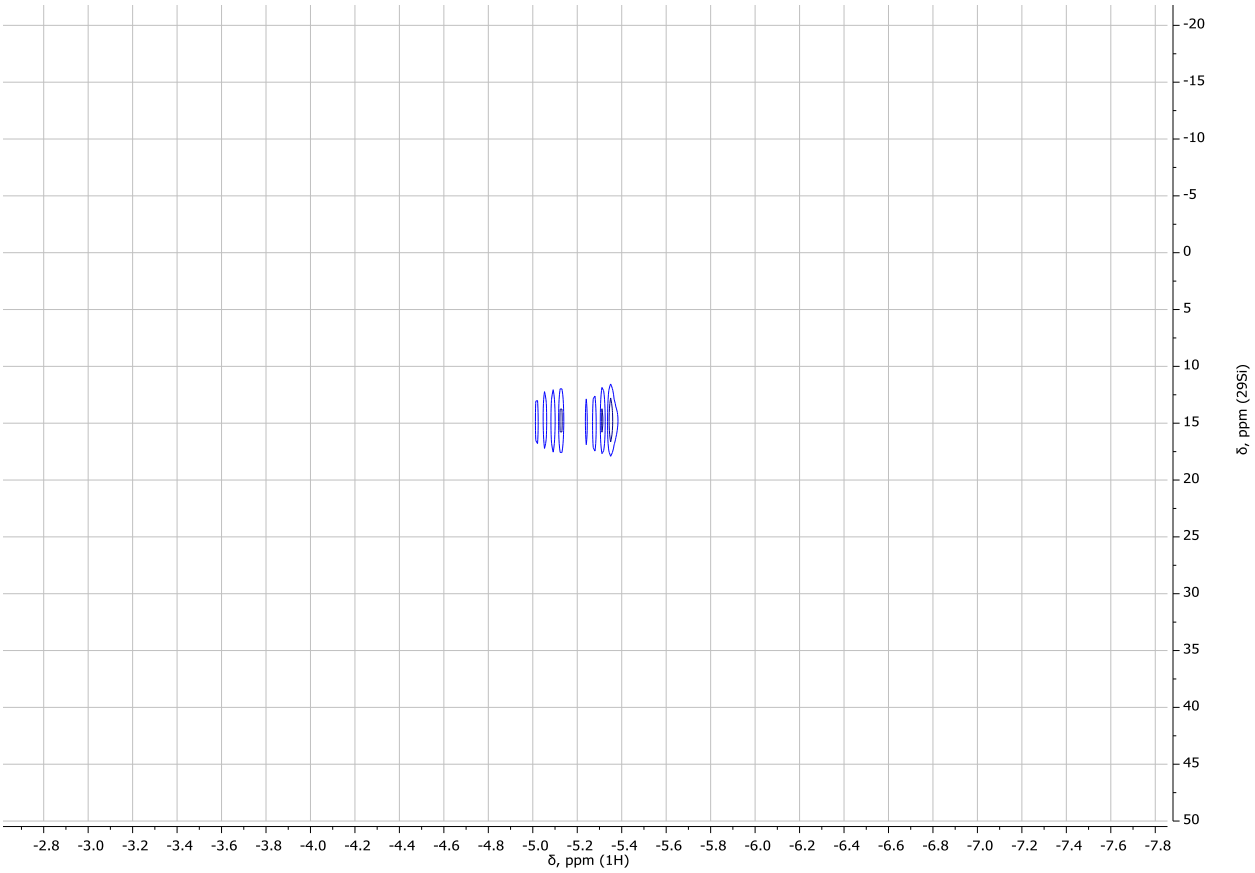

Figure S4. ^{29}Si-^{1}H HSQC NMR (99 MHz, C_6D_6) spectrum of (SiNP)Rh(COE) (**5**).

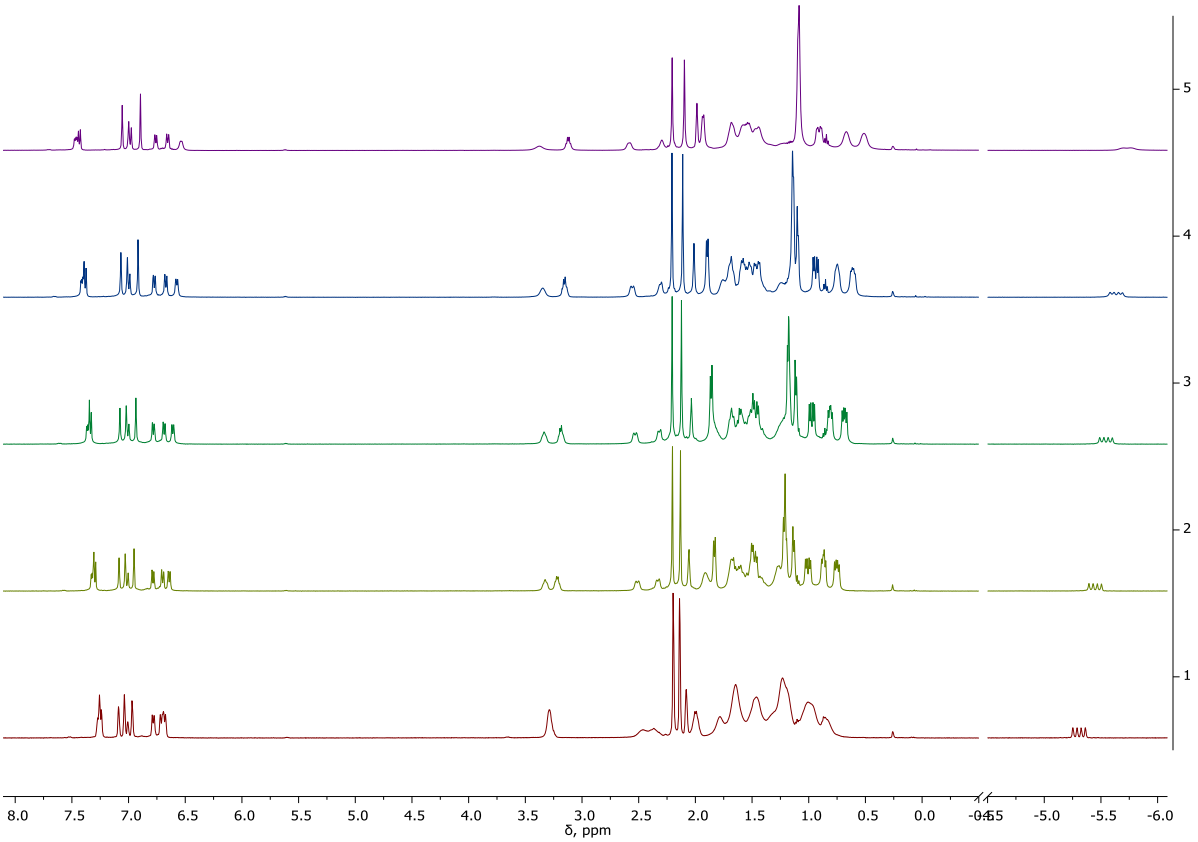

Figure S5. ^{1}H NMR (500 MHz, C_7D_8) spectrum of (SiNP)Rh(COE) (**5**) at various temperatures (bottom to top): 25 ºC, -5 ºC, -25 ºC, -45 ºC, and -65 ºC.

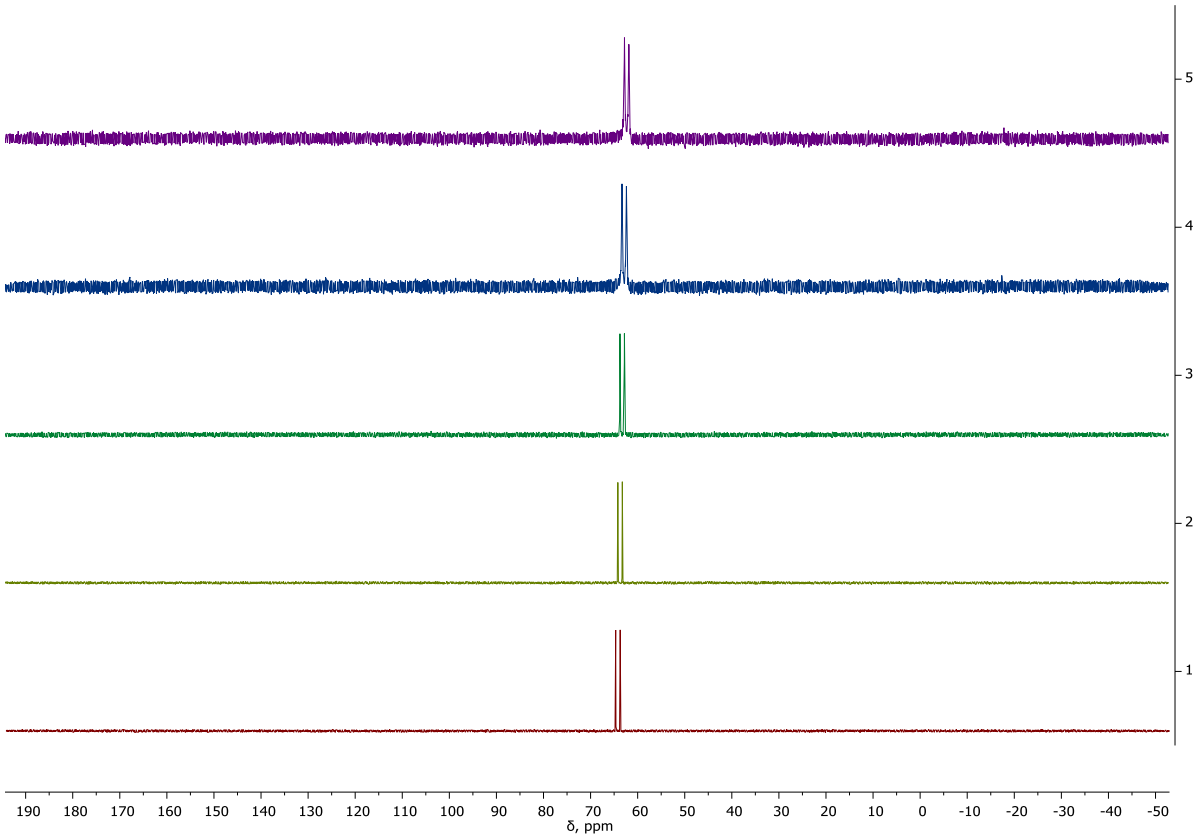

Figure S6. $^{31}P\{^{1}H\}$ NMR (500 MHz, C_7D_8) spectrum of (SiNP)Rh(COE) (**5**) at various temperatures (bottom to top): 25 ºC, -5 ºC, -25 ºC, -45 ºC, and -65 ºC.

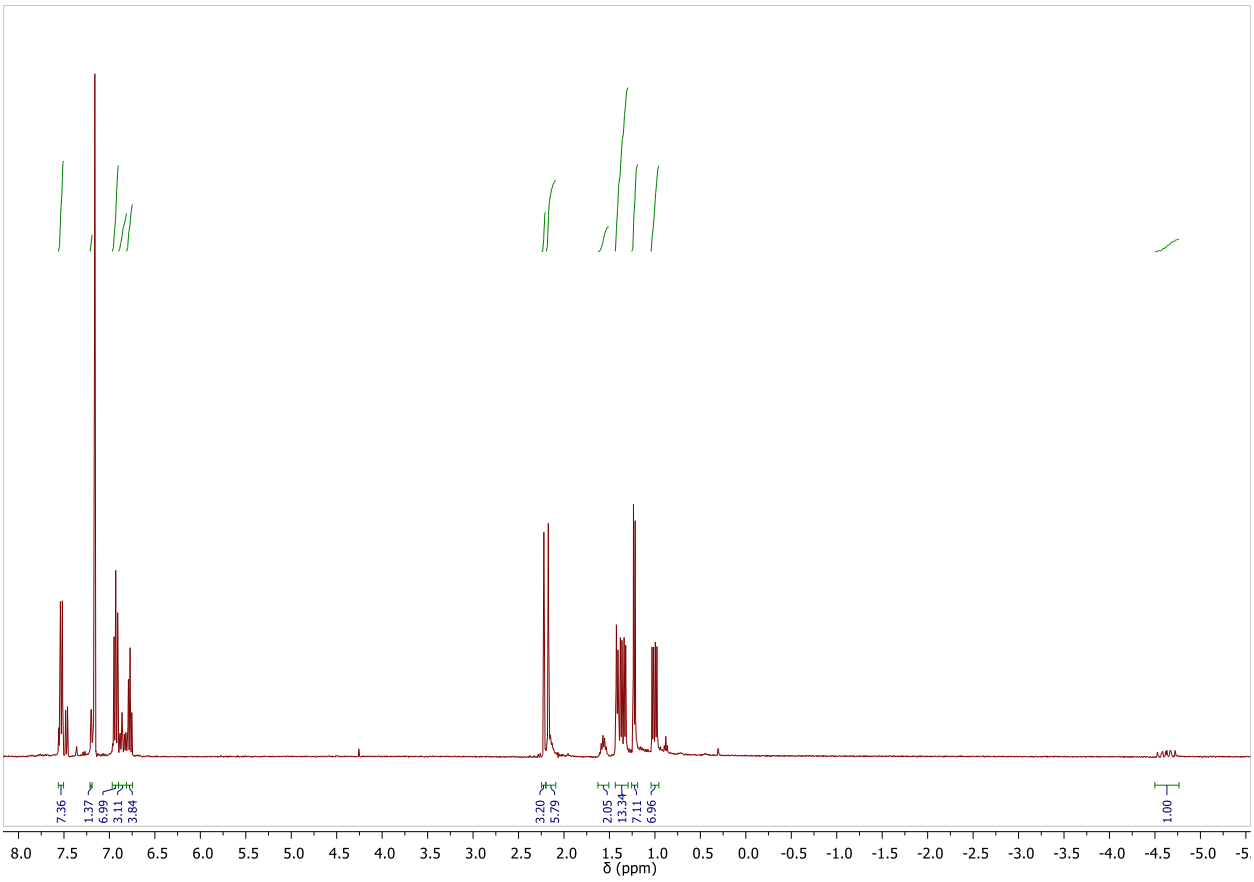

Figure S7. ^{1}H NMR (400 MHz, C_6D_6) spectrum of (SiNP)Rh(P(OPh)$_3$) (**6**).

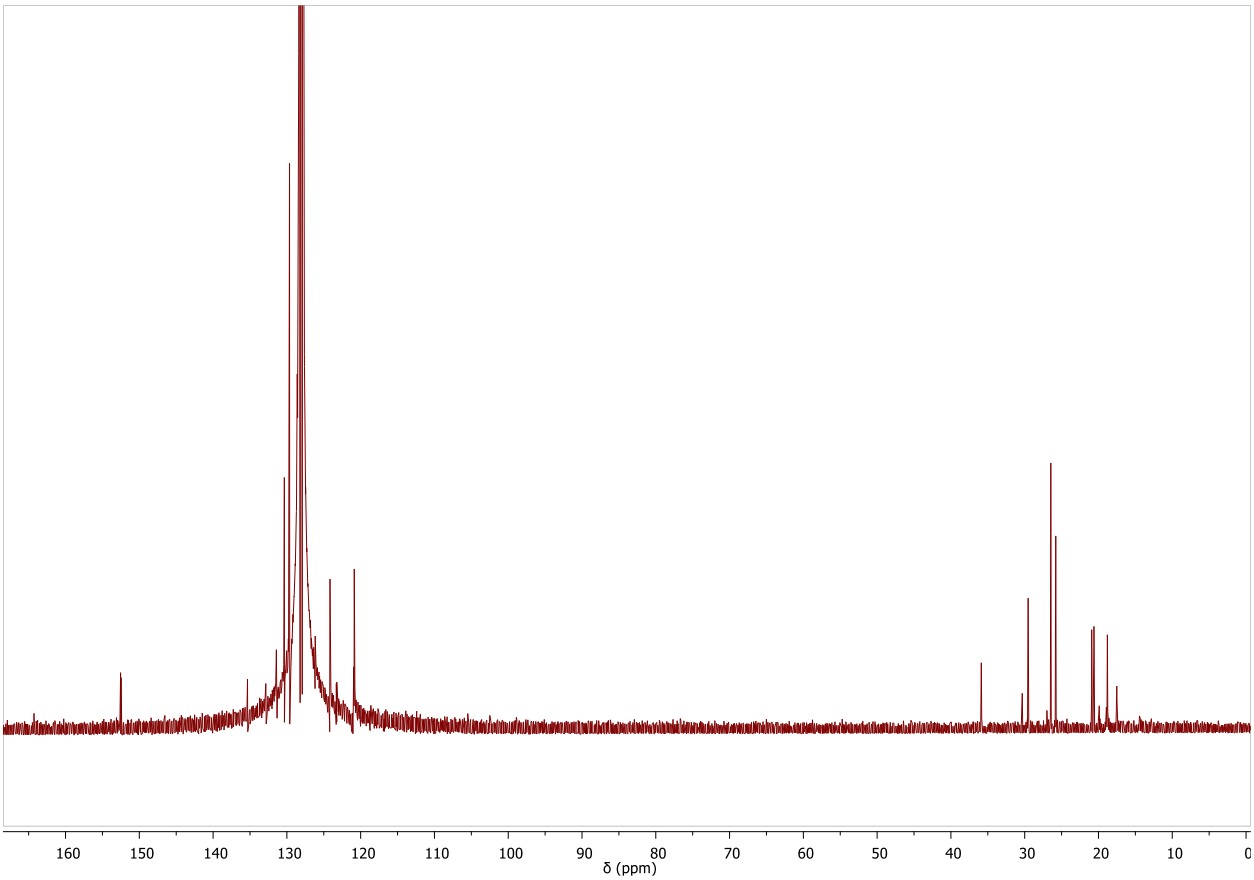

Figure S8. $^{13}C\{^{1}H\}$ NMR (100 MHz, C_6D_6) spectrum of (SiNP)Rh($P(OPh)_3$) (**6**).

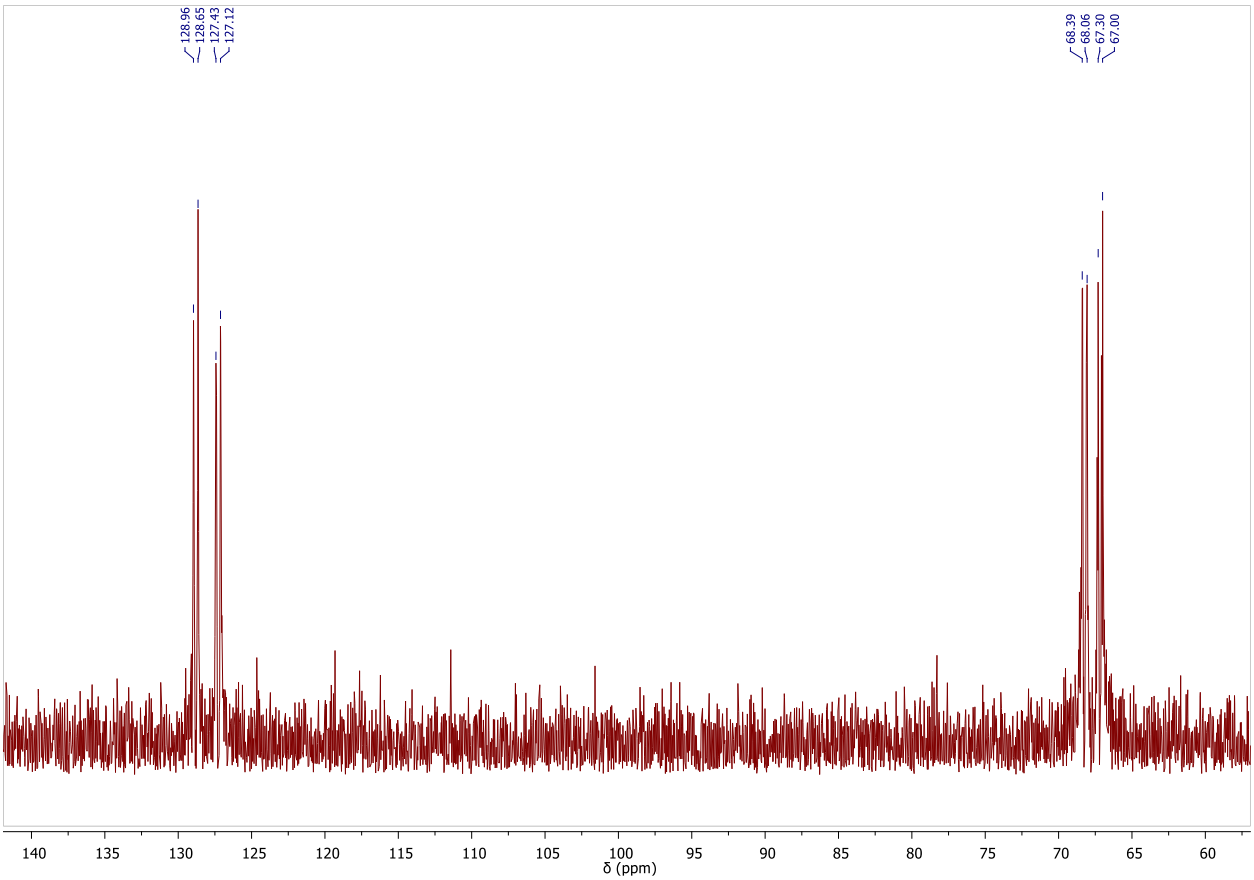

Figure S9. $^{31}P\{^{1}H\}$ NMR (162 MHz, C_6D_6) spectrum of *in situ* generated (SiNP)Rh(P(OPh)$_3$) (**6**).

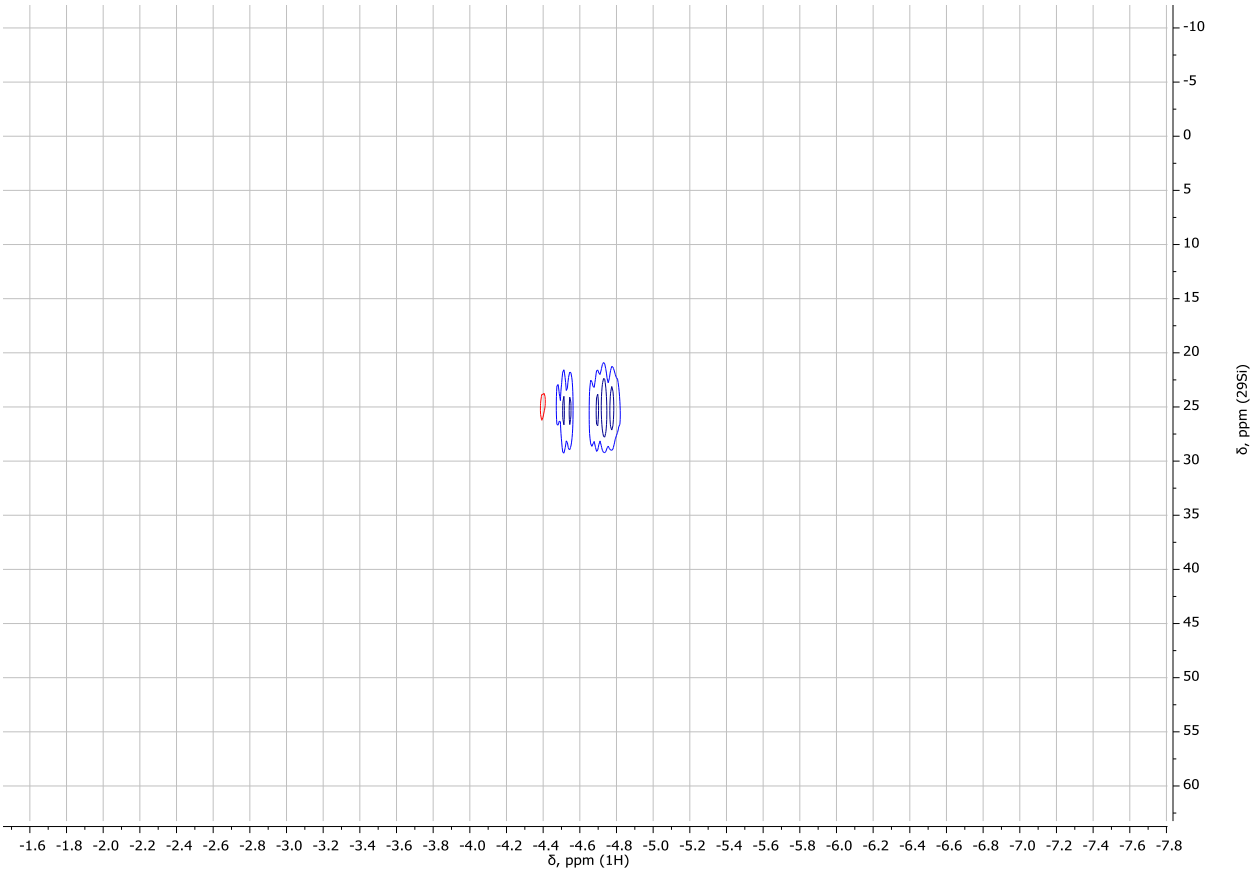

Figure S10. ^{29}Si-^{1}H HSQC NMR (99 MHz, C_6D_6) spectrum of *in situ* generated (SiNP)Rh(P(OPh)$_3$) (**6**).

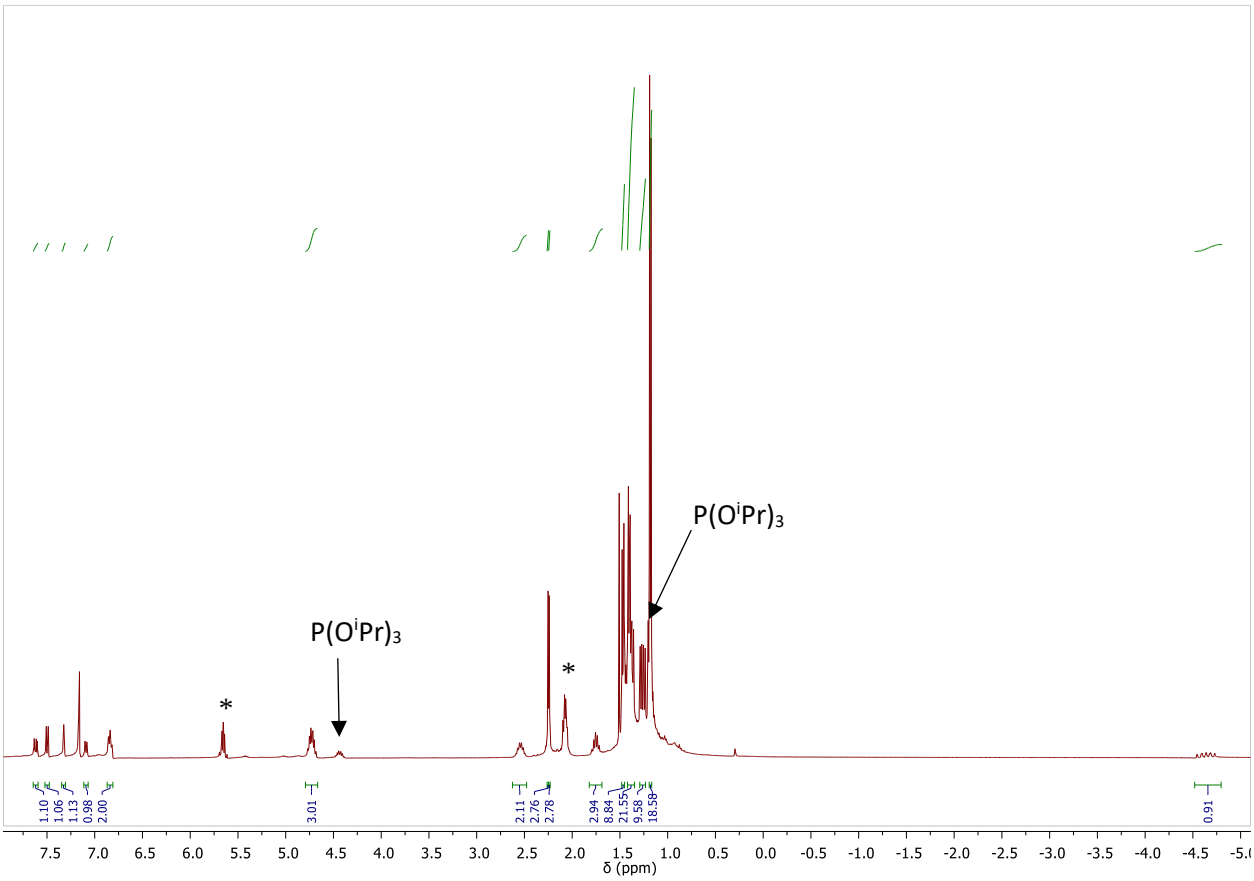

Figure S11. ^{1}H NMR (400 MHz, C_6D_6) spectrum of *in situ* generated (SiNP)Rh(P(O^{i}Pr)$_3$) (**7**). Sample contains residual silicone grease. Analysis was performed on an *in situ* sample and contains unidentified compounds in solution. Resolved cyclooctene peaks are denoted by *.

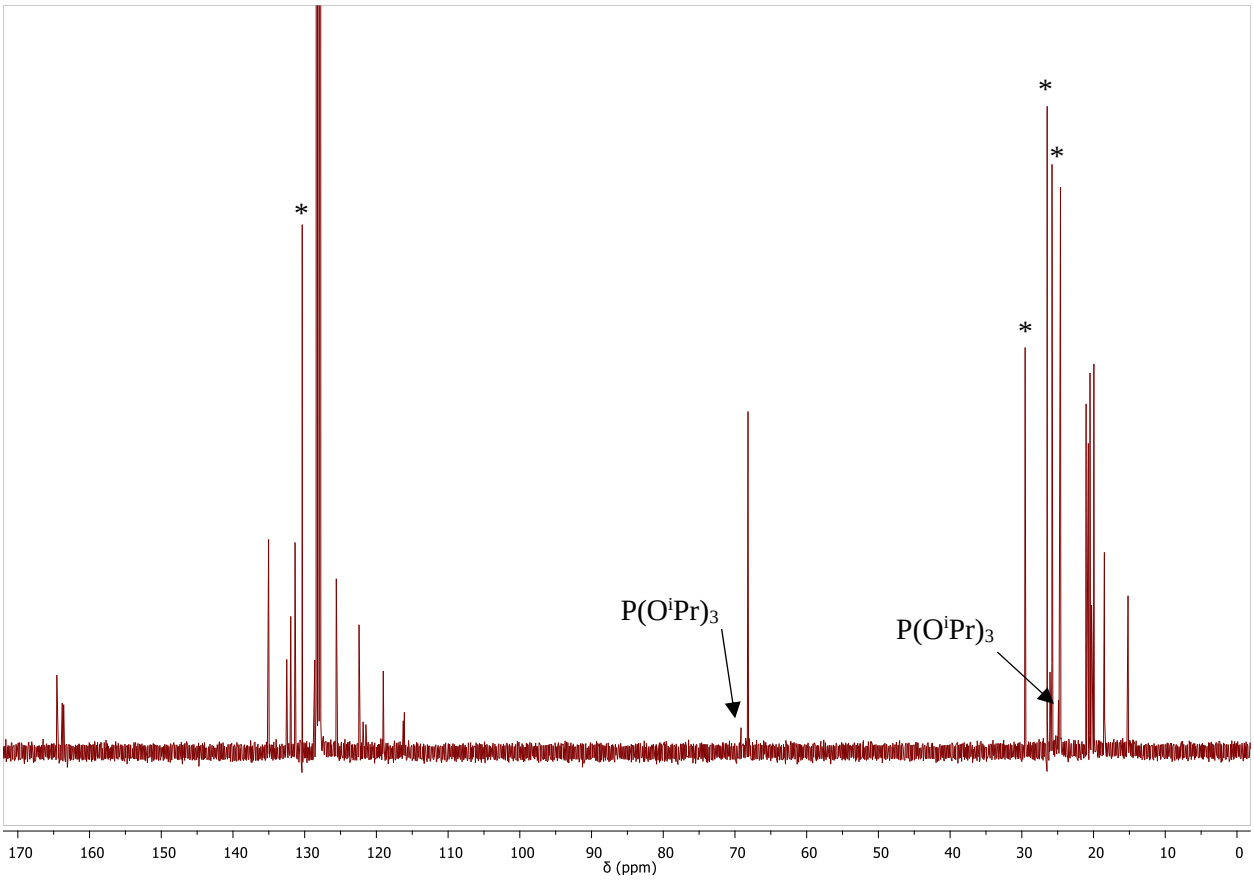

Figure S12. $^{13}C\{^{1}H\}$ NMR (100 MHz, C_6D_6) spectrum of *in situ* generated (SiNP)Rh($P(O^iPr)_3$) (**7**). Analysis was performed on an *in situ* sample and contains unidentified compounds in solution. Cyclooctene is denoted by *.

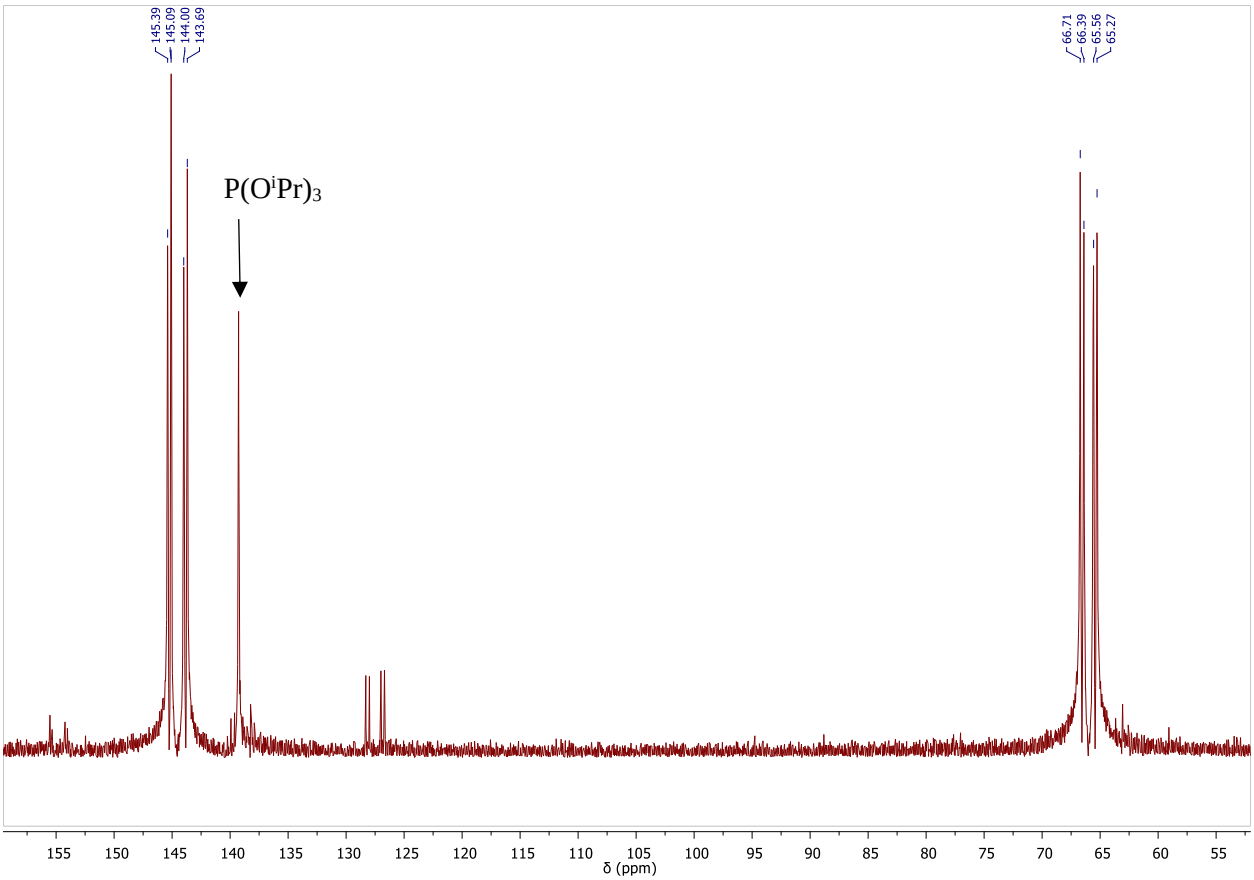

Figure S13. $^{31}P\{^{1}H\}$ NMR (162 MHz, C_6D_6) spectrum of *in situ* generated (SiNP)Rh($P(O^iPr)_3$) (**7**). Analysis was performed on an *in situ* sample and contains unidentified compounds in solution.

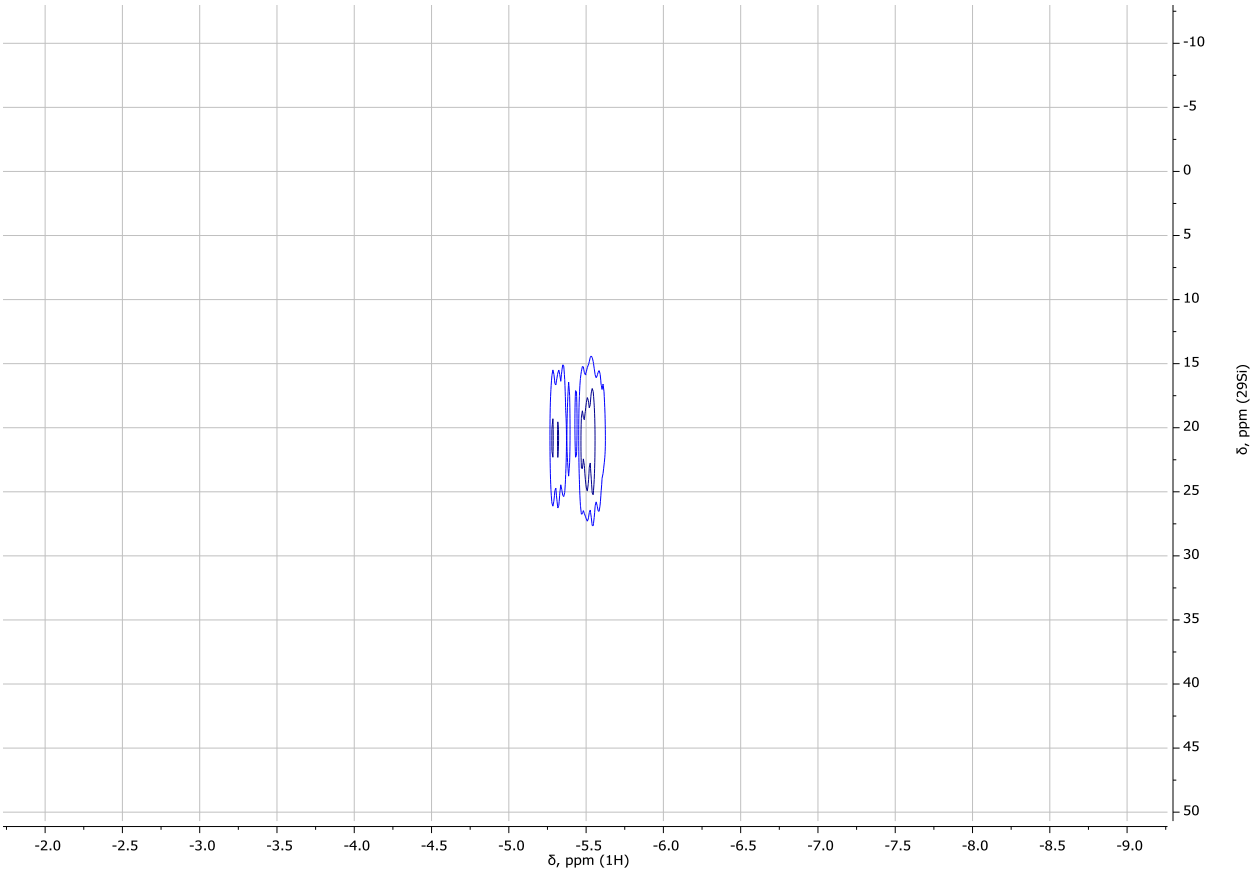

Figure S14. ^{29}Si-^{1}H HSQC NMR (99 MHz, C_6D_6) spectrum of *in situ* generated (SiNP)Rh(P(O^{i}Pr)$_3$) (**7**).

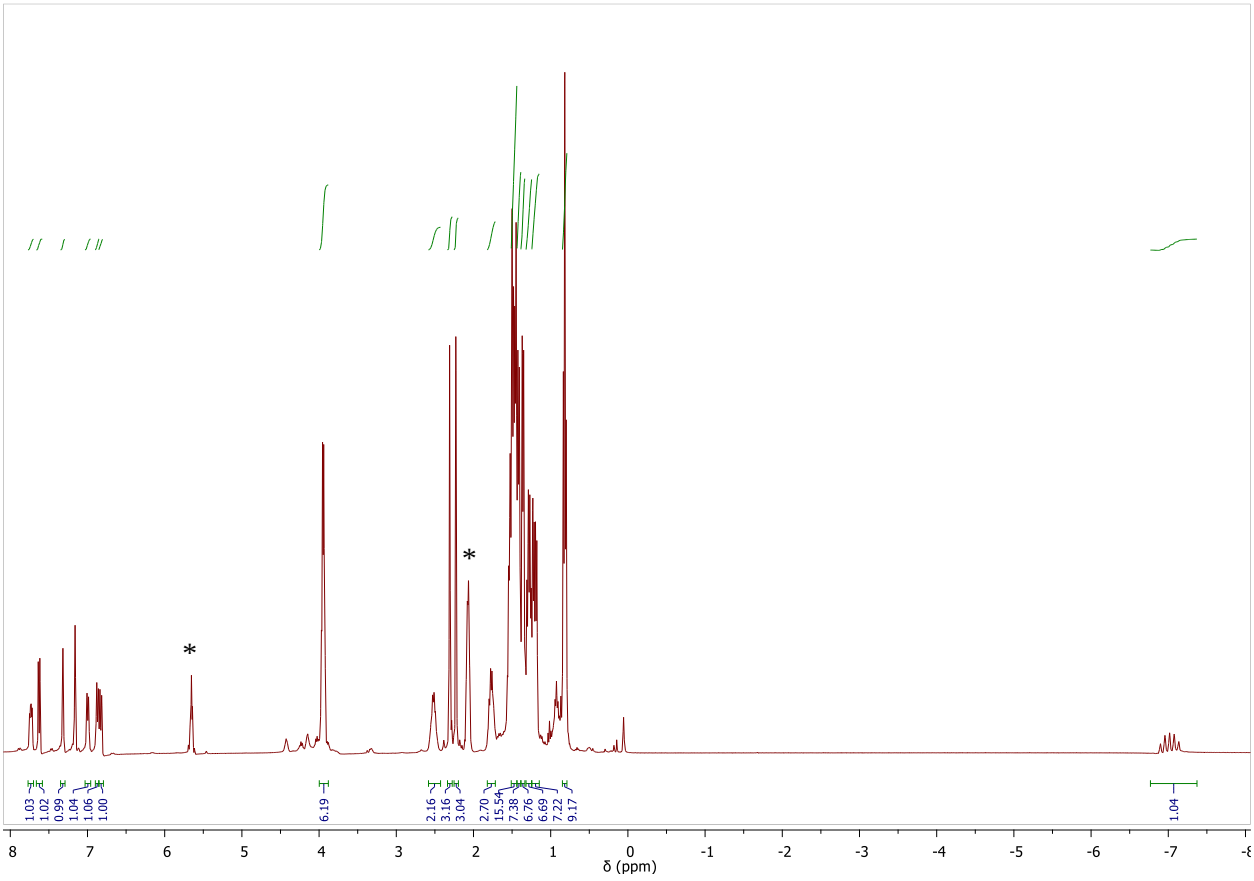

Figure S15. ^{1}H NMR (400 MHz, C_6D_6) spectrum of *in situ* generated (SiNP)Rh(P(OBu)$_3$) (**8**). Analysis was performed on an *in situ* sample and contains unidentified compounds in solution. Resolved cyclooctene peaks are denoted by *.

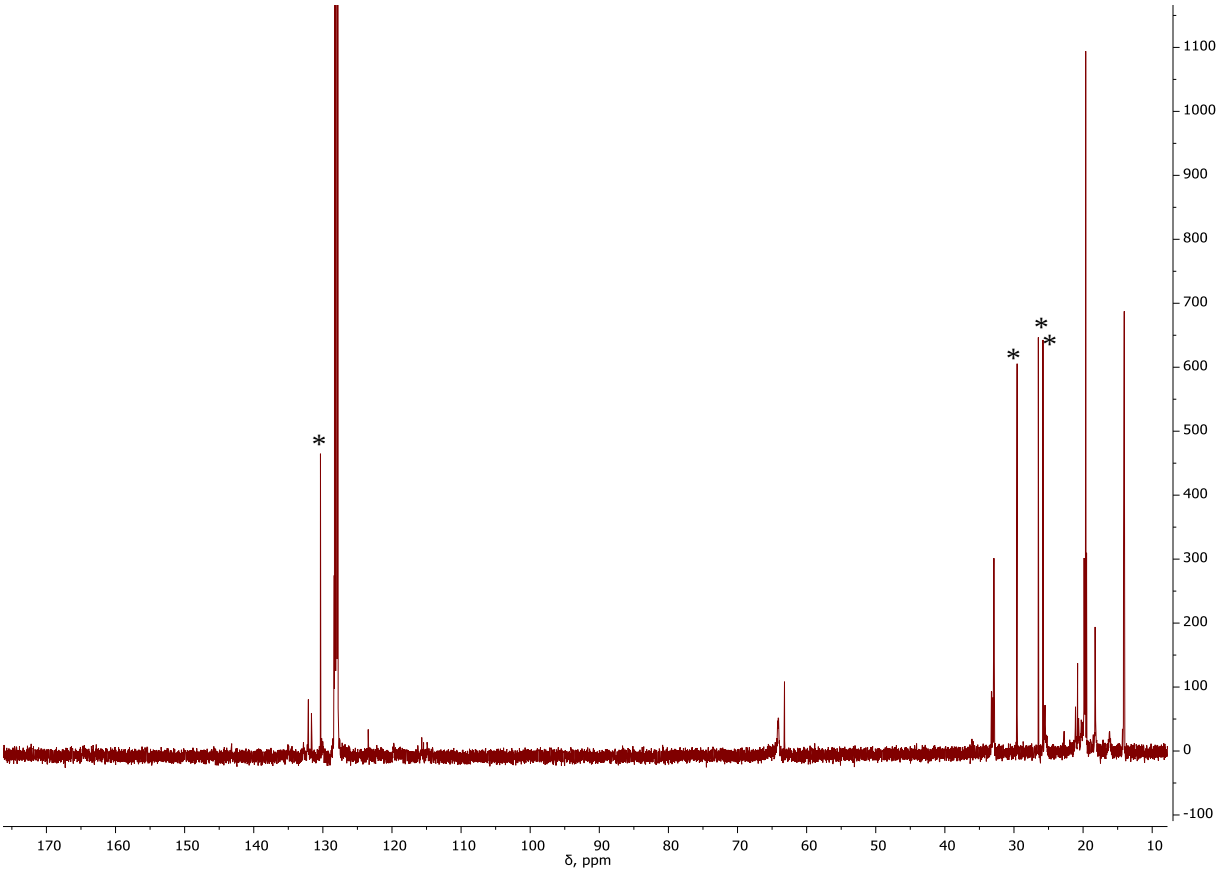

Figure S16. $^{13}C\{^{1}H\}$ NMR (100 MHz, C_6D_6) spectrum of *in situ* generated (SiNP)Rh(P(OBu)$_3$) (**8**). Analysis was performed on an *in situ* sample and contains unidentified compounds in solution. Resolved cyclooctene peaks are denoted by *.

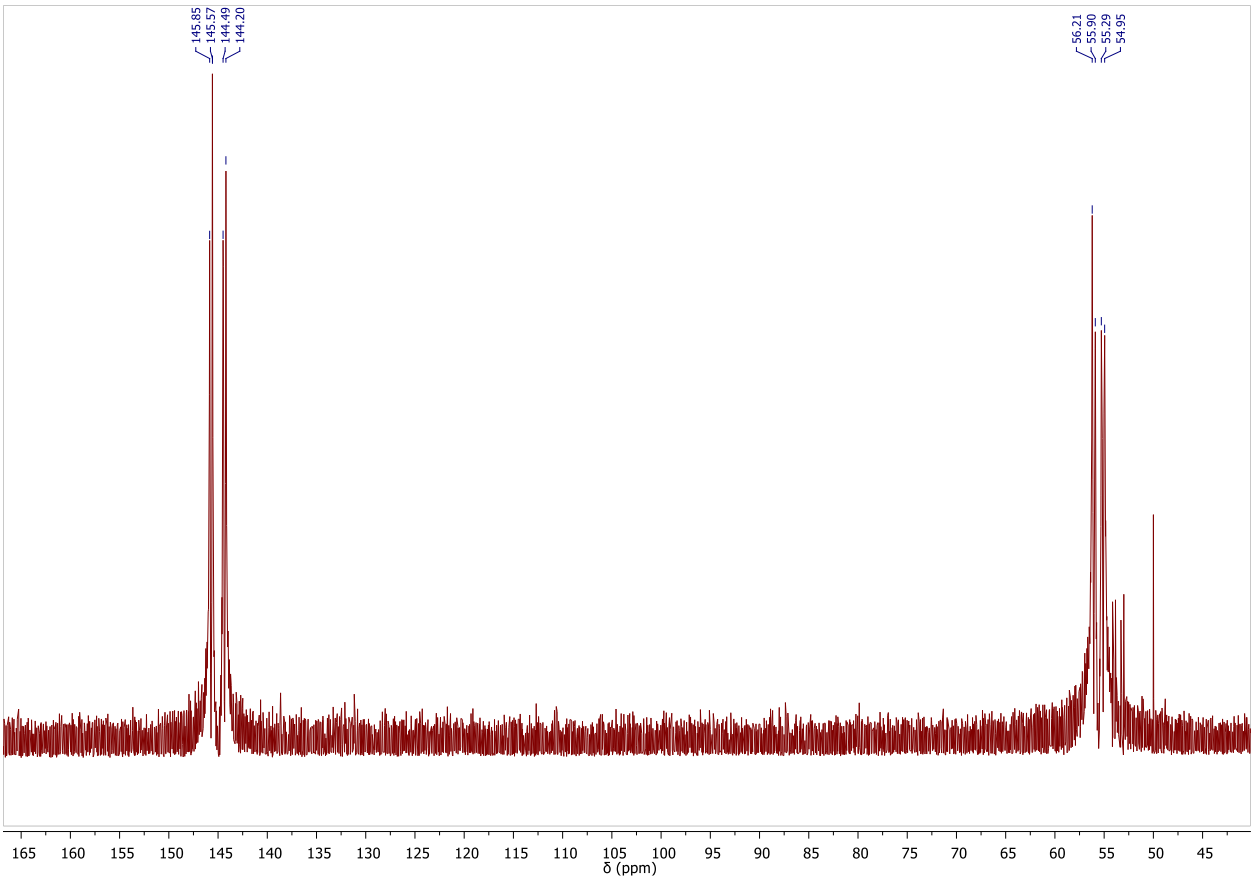

Figure S17. $^{31}P\{^{1}H\}$ NMR (162 MHz, C_6D_6) spectrum of *in situ* generated (SiNP)Rh(P(OBu)$_3$) (**8**). Analysis was performed on an *in situ* sample and contains unidentified compounds in solution.

Figure S18. ^{29}Si-^{1}H HSQC NMR (99 MHz, C_6D_6) spectrum of *in situ* generated (SiNP)Rh(P(OBu)$_3$) (**8**).

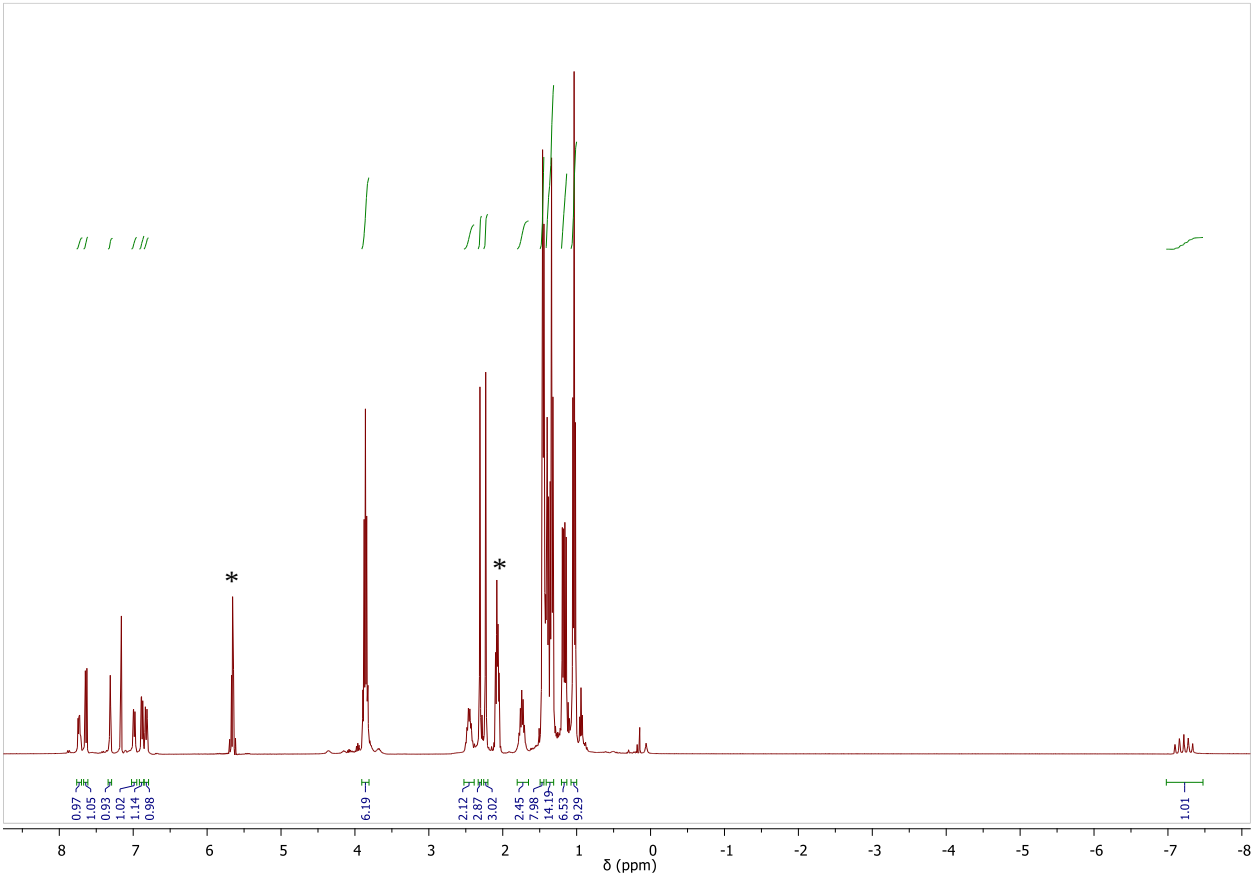

Figure S19. ^{1}H NMR (400 MHz, C_6D_6) spectrum of *in situ* generated (SiNP)Rh(P(OEt)$_3$) (**9**). Analysis was performed on an *in situ* sample and contains unidentified compounds in solution. Resolved cyclooctene peaks are denoted by *.

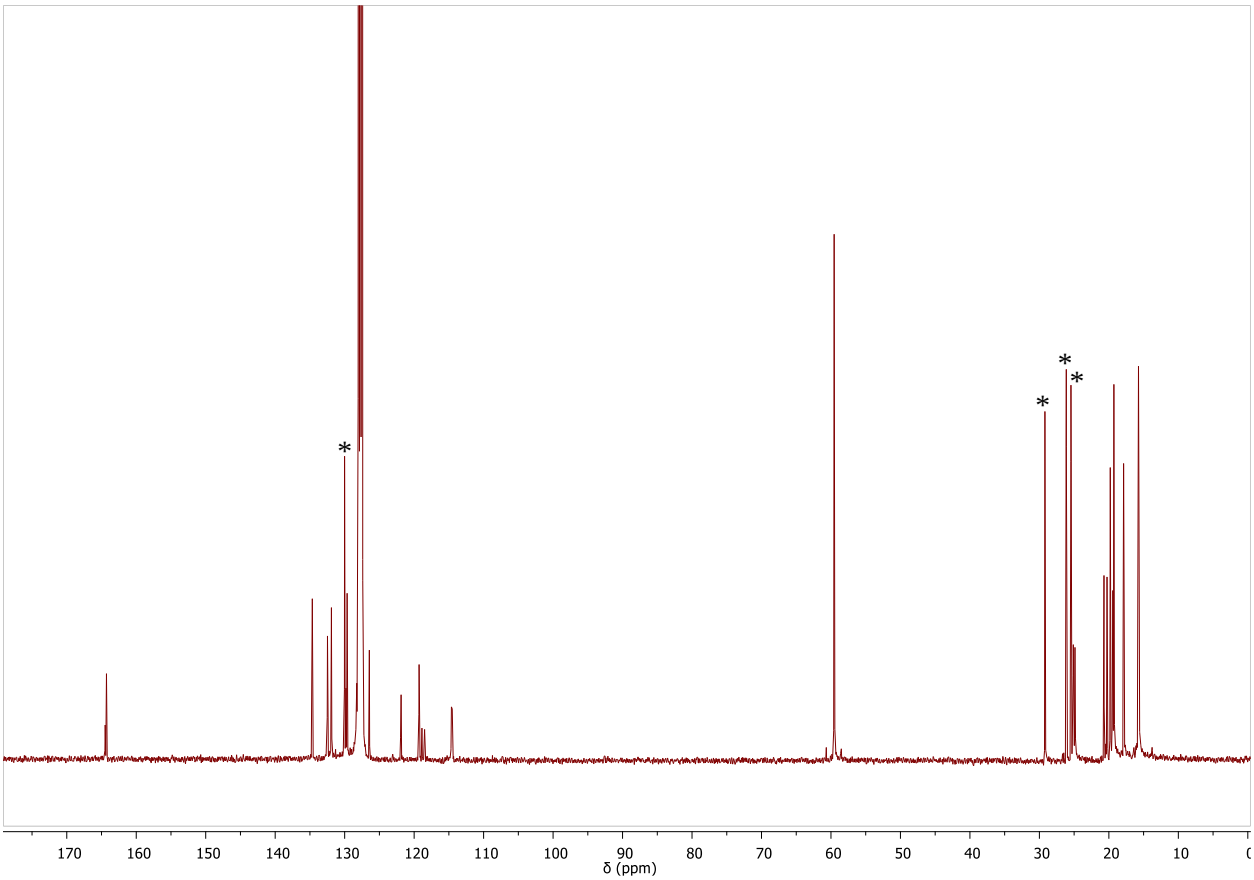

Figure S20. $^{13}C\{^{1}H\}$ NMR (100 MHz, C_6D_6) spectrum of *in situ* generated (SiNP)Rh(P(OEt)$_3$) (**9**). Analysis was performed on an *in situ* sample and contains unidentified compounds in solution. Resolved cyclooctene peaks are denoted by *.

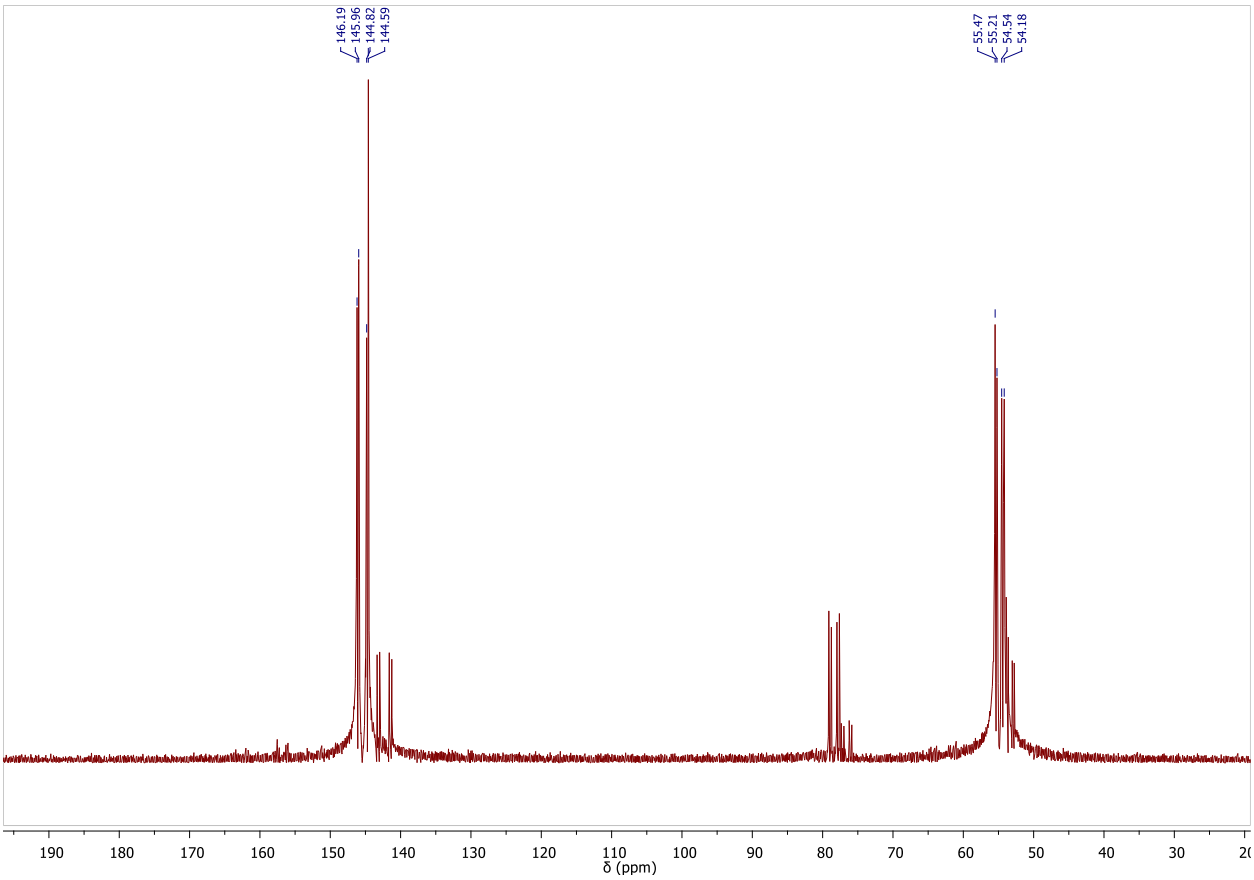

Figure S21. $^{31}P\{^{1}H\}$ NMR (162 MHz, C_6D_6) spectrum of *in situ* generated (SiNP)Rh($P(OEt)_3$) (**9**). Analysis was performed on an *in situ* sample and contains unidentified compounds in solution.

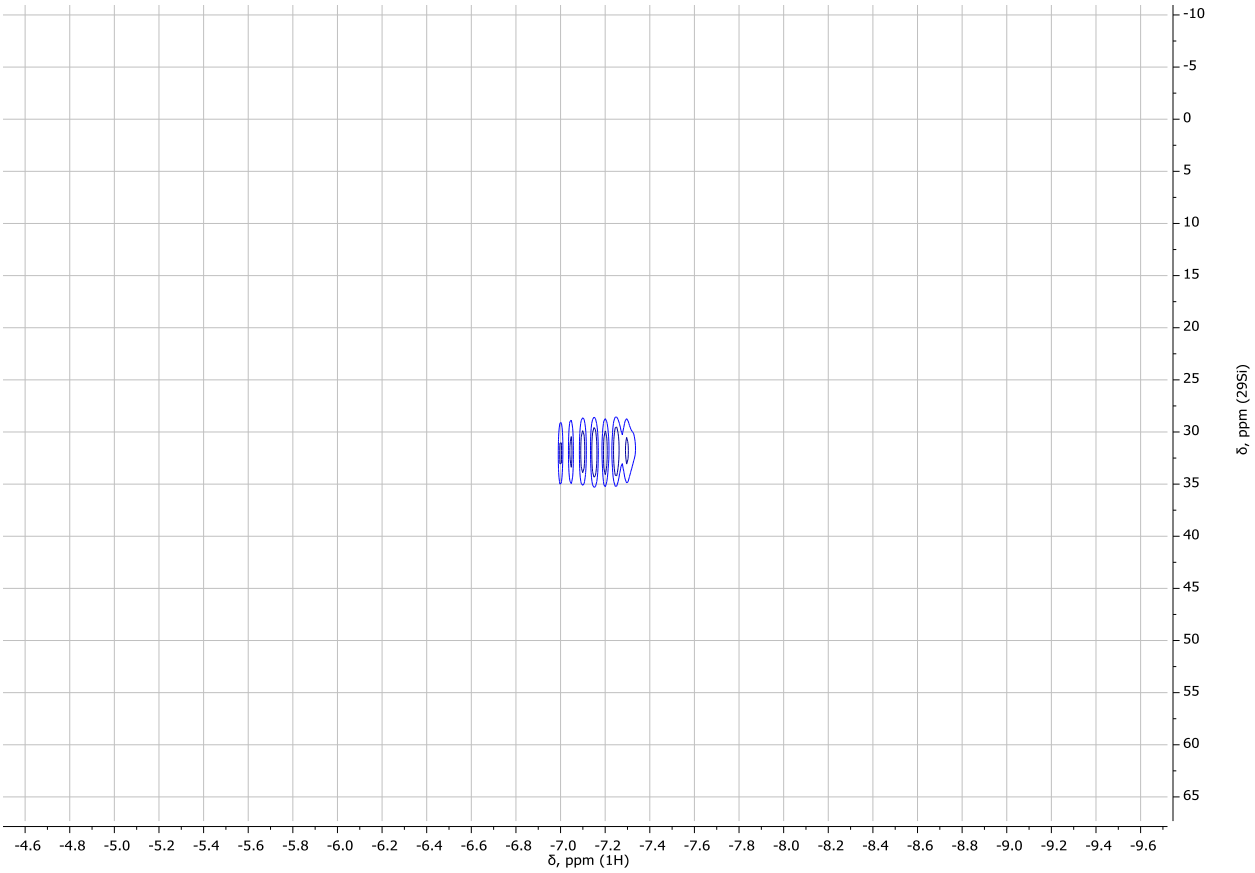

Figure S22. ^{29}Si-^{1}H HSQC NMR (99 MHz, C_6D_6) spectrum of *in situ* generated (SiNP)Rh(P(OEt)$_3$) (**9**).

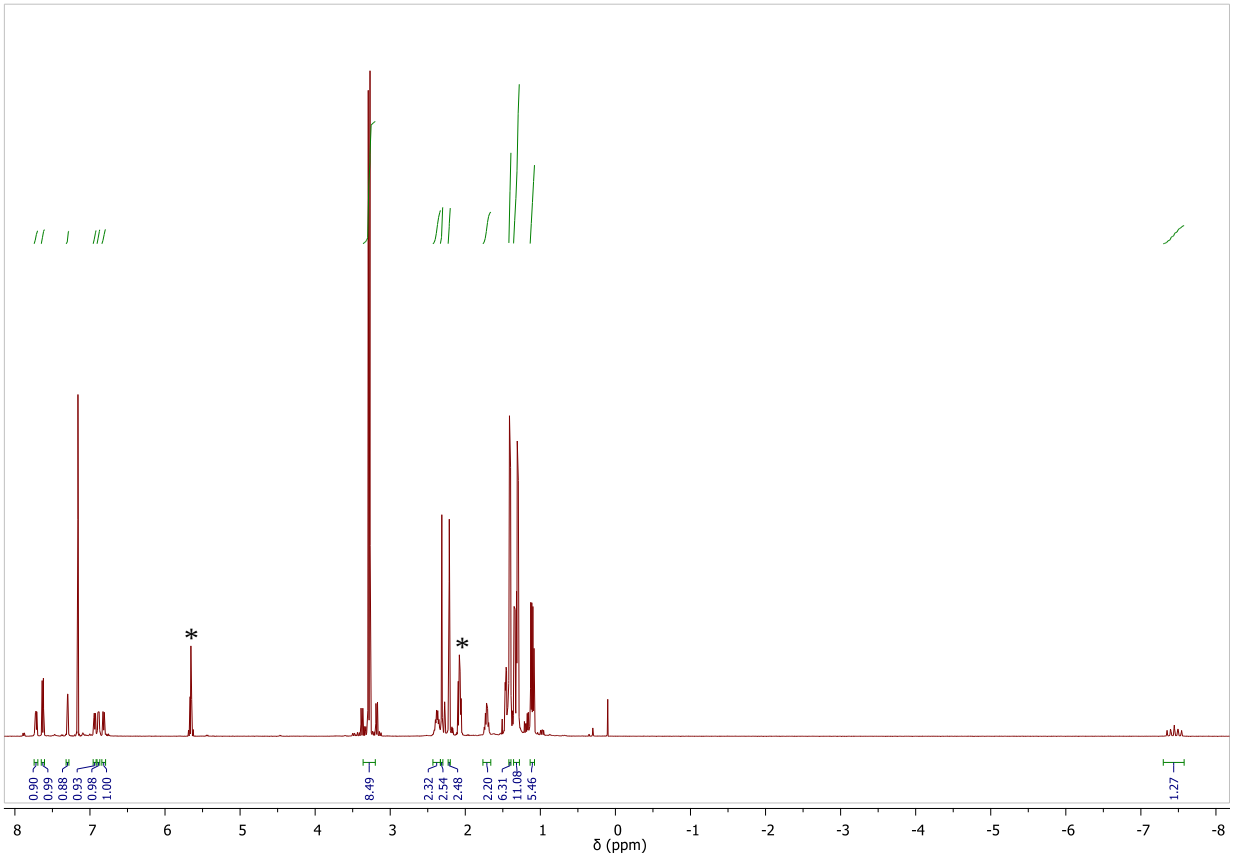

Figure S23. ^{1}H NMR (500 MHz, C_6D_6) spectrum of *in situ* generated (SiNP)Rh(P(OMe)$_3$) (**10**). Sample contains trace amounts of residual silicone grease. Analysis was performed on an *in situ* sample and contains unidentified compounds in solution. Resolved cyclooctene peaks are denoted by *.

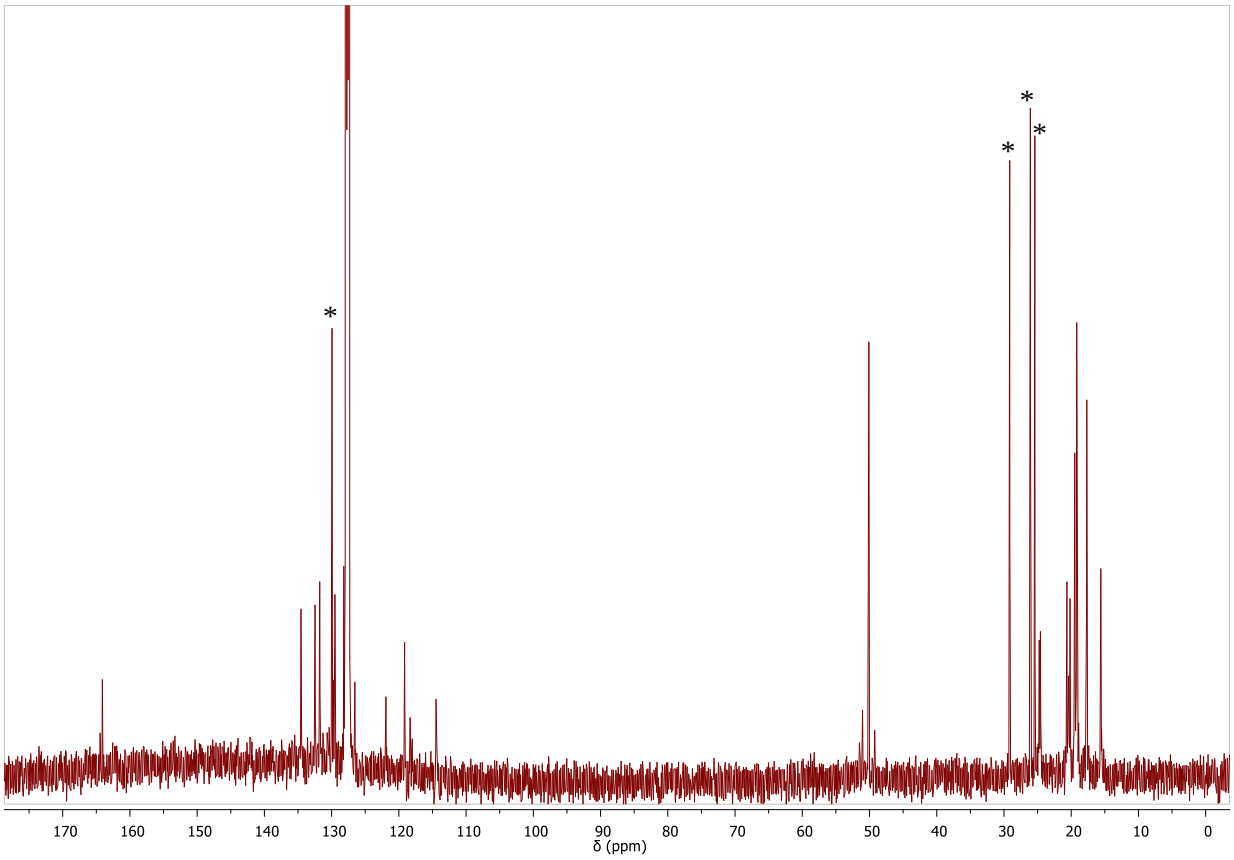

Figure S24. $^{13}C\{^{1}H\}$ NMR (128 MHz, C_6D_6) spectrum of *in situ* generated (SiNP)Rh(P(OMe)$_3$) (**10**). Analysis was performed on an *in situ* sample and contains unidentified compounds in solution. Resolved cyclooctene peaks are denoted by *.

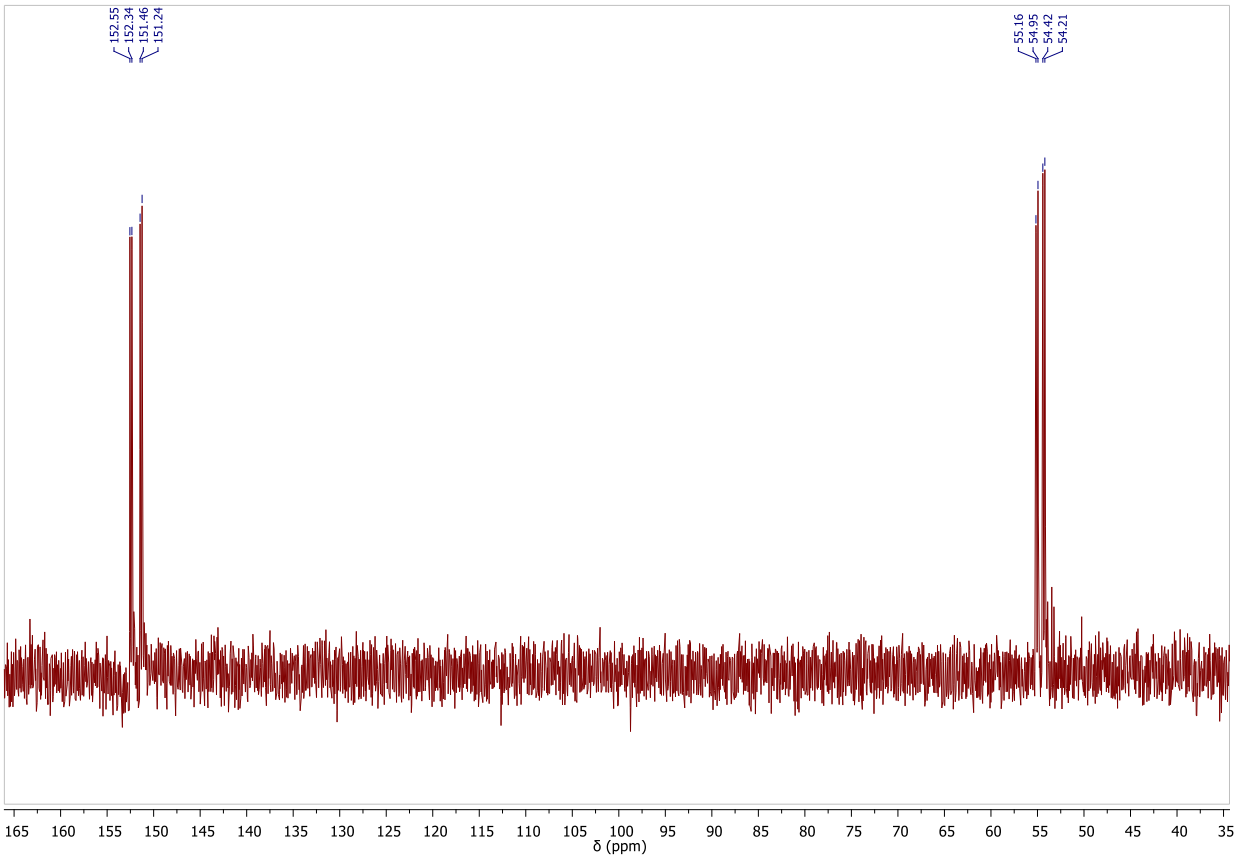

Figure S25. $^{31}P\{^{1}H\}$ NMR (202 MHz, C_6D_6) spectrum of *in situ* generated (SiNP)Rh(P(OMe)$_3$) (**10**). Analysis was performed on an *in situ* sample and contains unidentified compounds in solution.

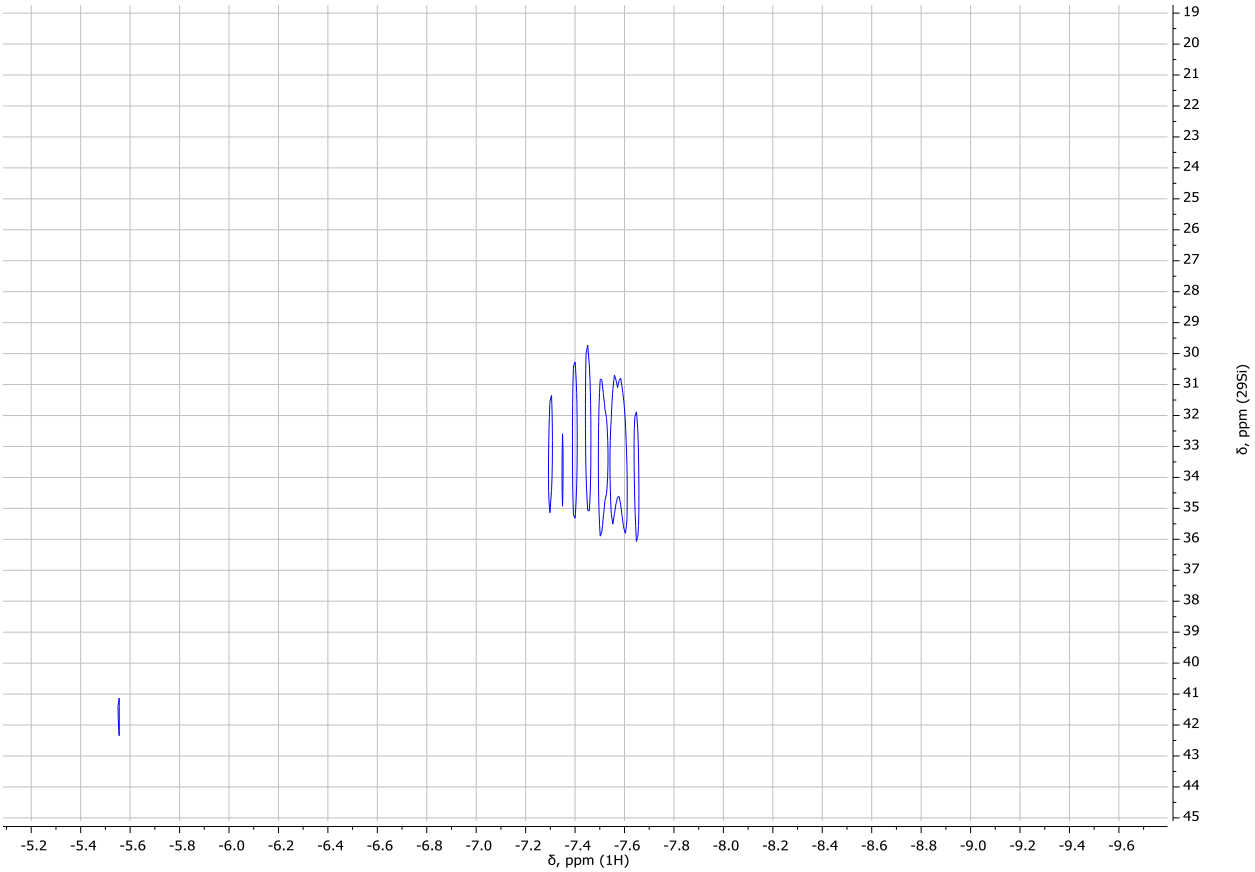

Figure S26. ^{29}Si-^{1}H HSQC NMR (99 MHz, C_6D_6) spectrum of *in situ* generated (SiNP)Rh(P(OMe)$_3$) (**10**).

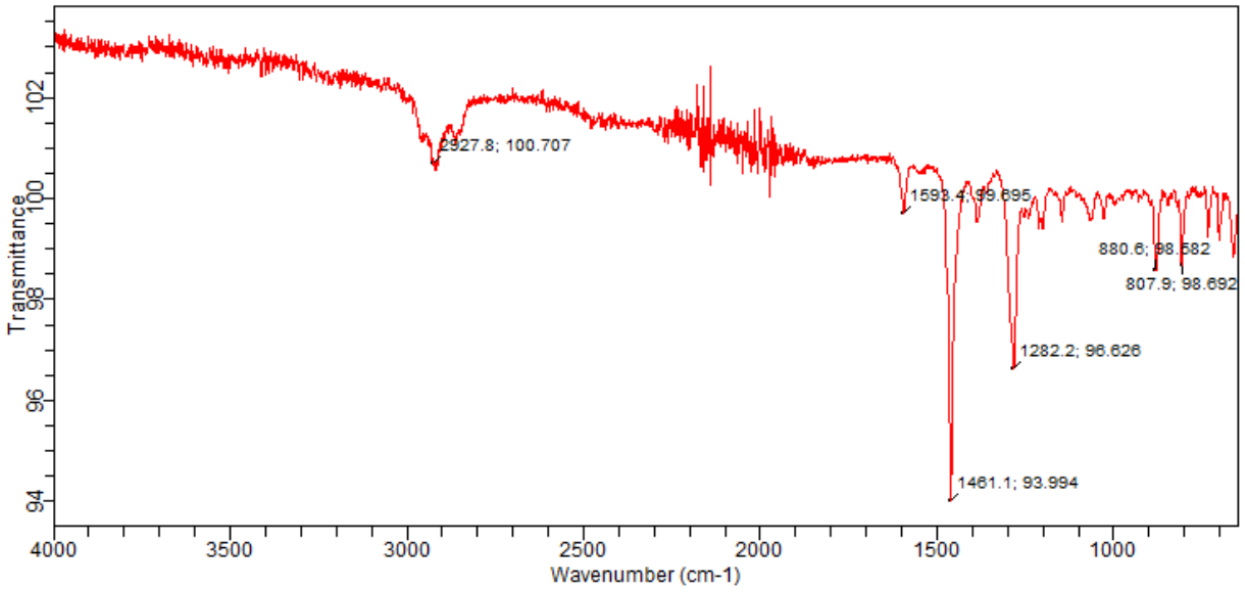

Figure S27. IR spectrum of (SiNP)Rh(COE) (**5**) in C_6D_6.

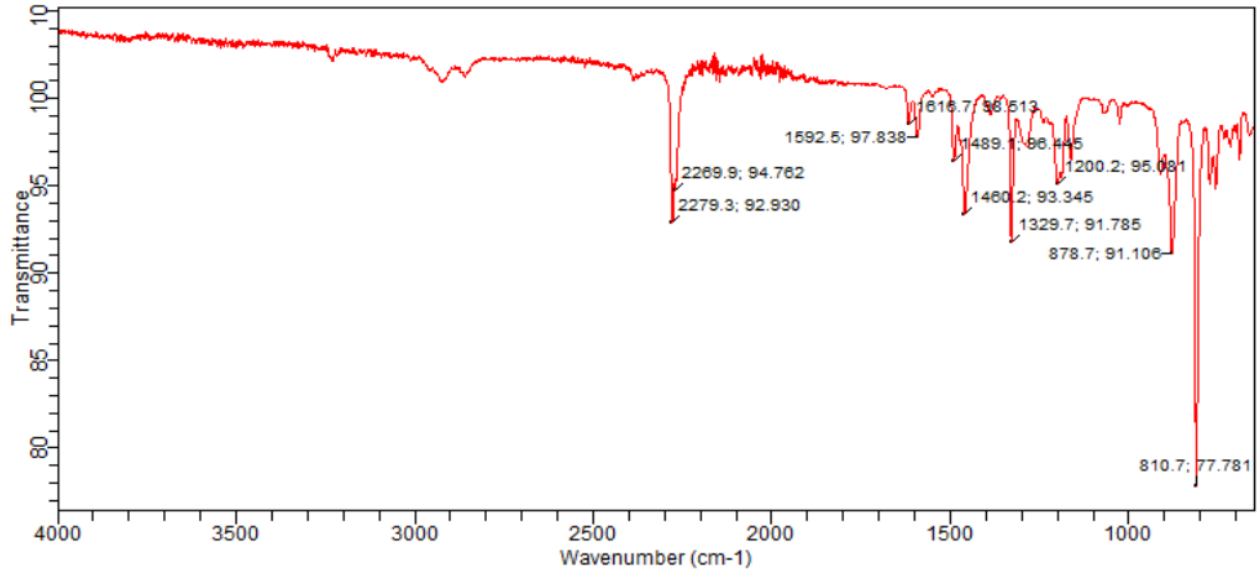

Figure S28. IR spectrum of (SiNP)Rh(P(OPh)$_3$) (**6**) in C_6D_6. Absorbances around 2279 cm^{-1} belong to the C-D stretching frequency of C_6D_6.

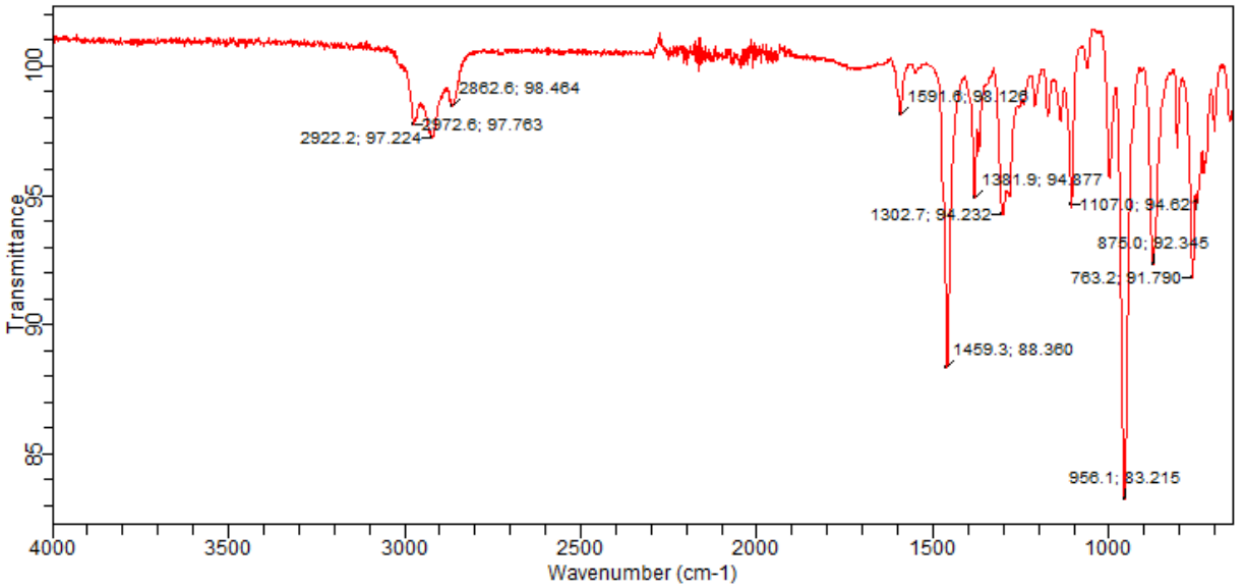

Figure S29. IR spectrum of (SiNP)Rh(P(O^{i}Pr)$_3$) (**7**) in C_6D_6.

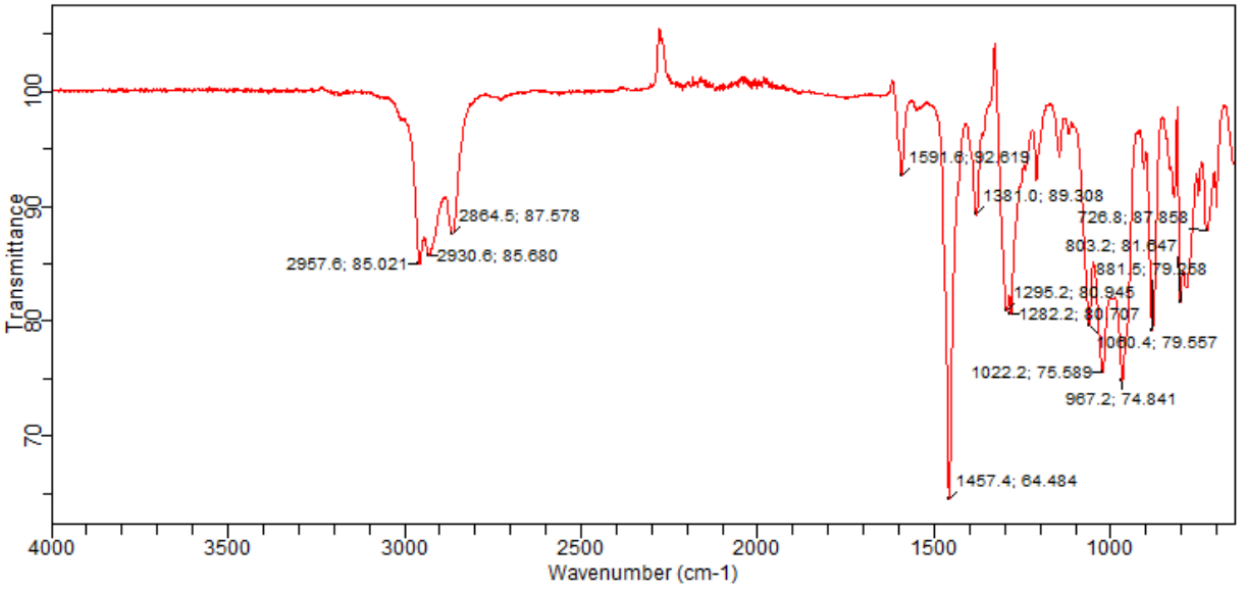

Figure S29. IR spectrum of (SiNP)Rh(P(OBu)$_3$) (**8**) in C_6D_6.

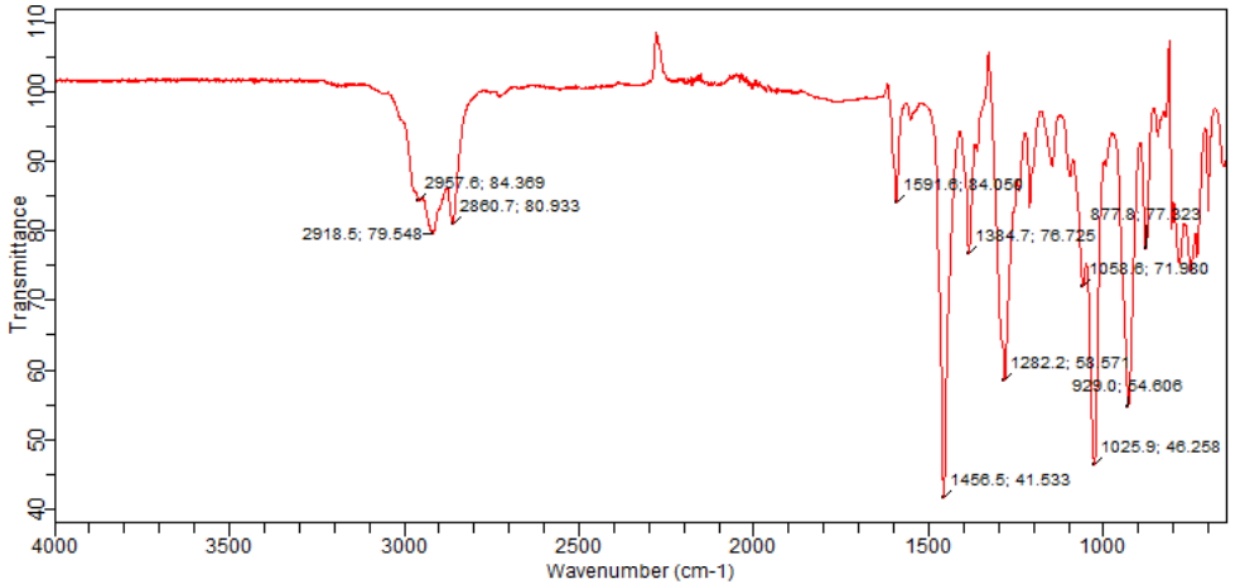

Figure S30. IR spectrum of (SiNP)Rh(P(OEt)$_3$) (**9**) in C_6D_6.

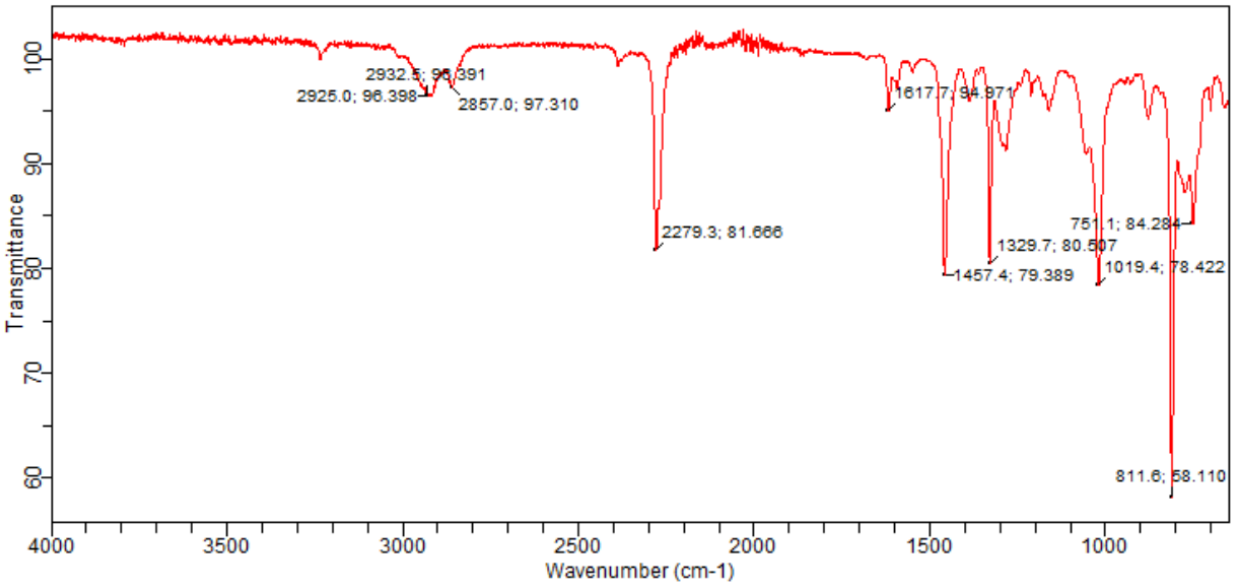

Figure S31. IR spectrum of (SiNP)Rh(P(OMe)$_3$) (**10**) in C_6D_6. Absorbances around 2279 cm^{-1} belong to the C-D stretching frequency of C_6D_6.

2. X-ray Diffractometry Details.

X-Ray data collection, solution, and refinement for compound 6. CCDC #1894481

An orange, multi-faceted block of suitable size (0.230 x 0.193 x 0.116 mm^3) and quality was selected from a representative sample of crystals of the same habit using an optical microscope, mounted onto a Mitegen MicroLoops™ (MiTeGen, LLC., Ithaca, NY) and placed in a cold nitrogen stream of nitrogen. Low temperature (100 K) X-ray data were obtained on a Bruker Smart Breeze CCD diffractometer (Mo sealed X-ray tube, K_α = 0.71073 Å). All diffractometer manipulations, including data collection, integration and scaling were carried out using the Bruker APEXII software.[1]

Integrated intensity information for each reflection was obtained by reduction of the data frames with the program APEX3.[2] The integration method employed a three dimensional profiling algorithm and all data were corrected for Lorentz and polarization factors, as well as for crystal decay effects. Finally the data was merged and scaled to produce a suitable data set. The absorption correction program SADABS.[3] was employed to correct the data for absorption effects.

Systematic reflection conditions and statistical tests of the data suggested the space group $P2_12_12_1$. A solution was obtained readily using XT/XS in APEX3.[2, 4] Hydrogen atoms were placed in idealized positions and were set riding on the respective parent atoms. All non-hydrogen atoms were refined with anisotropic thermal parameters. Bridging hydrogen (H1) was added based on the weak residual electron density. Restrain was added to keep this hydrogen from drifting. Absence of additional symmetry and voids were confirmed using PLATON (ADDSYM).[5] The structure was refined (weighted least squares refinement on F^2) to convergence.[4, 6]

X-Ray data collection, solution, and refinement for compound 10. CCDC # 2033844.

A Leica MZ 75 microscope was used to identify a brown block with very well defined faces with dimensions (max, intermediate, and min) 0.249 x 0.214 x 0.182 mm^3 from a representative sample of crystals of the same habit. The crystal mounted on a nylon loop was then placed in a cold nitrogen stream (Oxford) maintained at 110 K.

A BRUKER APEX 2 Duo X-ray (three-circle) diffractometer was employed for crystal screening, unit cell determination, and data collection. The goniometer was controlled using the APEX3 software suite, v2017.3-0.[2] The sample was optically centered with the aid of a video camera such that no translations were observed as the crystal was rotated through all positions. The detector (Bruker - PHOTON) was set at 6.0 cm from the crystal sample. The X-ray radiation employed was generated from a Mo sealed X-ray tube (Kα = 0.71073Å with a potential of 40 kV and a current of 40 mA).

45 data frames were taken at widths of 1.0°. These reflections were used in the auto-indexing procedure to determine the unit cell. A suitable cell was found and refined by nonlinear least squares and Bravais lattice procedures. The unit cell was verified by examination of the *h k l* overlays on several frames of data. No super-cell or erroneous reflections were observed.

After careful examination of the unit cell, an extended data collection procedure (6 sets) was initiated using omega and phi scans.

Integrated intensity information for each reflection was obtained by reduction of the data frames with the program APEX3.[2] The integration method employed a three-dimensional profiling algorithm and all data were corrected for Lorentz and polarization factors, as well as for crystal decay effects. Finally, the data was merged and scaled to produce a suitable data set. The absorption correction program SADABS[3] was employed to correct the data for absorption effects.

Systematic reflection conditions and statistical tests of the data suggested the space group P-1. A solution was obtained readily (Z=4; Z'=2) using XT/XS in APEX2.[1,4] Hydrogen atoms were placed in idealized positions and were set riding on the respective parent atoms. All non-hydrogen atoms were refined with anisotropic thermal parameters. Elongated thermal ellipsoids on two of the isopropyl groups (C21-C23), (C24-C26) and one of the methoxy groups (O3-C29) indicated disorder and were modeled successfully between two positions each with an occupancy ratio of 0.55:0.45. Several other groups also indicated possible disorder. However, our trials did not improve the reliability factors and this latter disorder were not modeled. Appropriate restraints and constraints were added to keep the bond distances, angles, and thermal ellipsoids meaningful. Residual electron density maps indicated the bridging hydrogen atoms (H1 and H1B) between Rh and Si atoms. They were successfully refined for atom positions and isotropic thermal parameters, with minimal bond distance (SADI) restraints. Absence of additional symmetry and voids were confirmed using PLATON (ADDSYM).[5] The structure was refined (weighted least squares refinement on F2) to convergence.[4,6]

ORTEP-3 and POV-Ray were employed for the final data presentation and structure plots.[7,8]

3. Computational Details.

All computations were carried out with the Gaussian09 program.[9] All of the geometries were fully optimized in the gas phase by B3LYP[10] functional. The Los Alamos basis set (LANL2DZ) and the associated effective core potential (ECP) was used for Rh atom, and an all-electron 6-31G(d) basis set was used for the other atoms (one additional p function was added for the hydrogen atom directly on Rh). It should be noted for **10-B**, the [Si-Rh-H] unit was kept fixed during the geometry optimization in order to better reproduce the experimental structure. Larger basis set SDD for Rh and 6-311+G(2d,p) for the other atoms was then used for the NMR chemical shift calculation.

4. ESI References

[1] Bruker (2013), APEX2, SAINT and SADABS. Bruker AXS ins., Madison, Wisconsin, USA.

[2] APEX3 "Program for Data Collection on Area Detectors" BRUKER AXS Inc., 5465 East Cheryl Parkway, Madison, WI 53711-5373 USA

[3] SADABS, G. M. Sheldrick, "Program for Absorption Correction of Area Detector Frames", BRUKER AXS Inc., 5465 East Cheryl Parkway, Madison, WI 53711-5373 USA.

[4] (a) G. M. Sheldrick, *Acta Cryst.*, 2008, **A64**, 112-122. (b) G. M. Sheldrick, *Acta Cryst.*, 2015, **A71**, 3-8. (c) G. M. Sheldrick, *Acta Cryst.*, 2015, **C71**, 3-8. (d) XT, XS, BRUKER AXS Inc., 5465 East Cheryl Parkway, Madison, WI 537115373 USA.

[5] A. L. Spek, "PLATON - A Multipurpose Crystallographic Tool" J. Appl. Cryst. 2003, 36, 7-13.; A. L. Spek, Utrecht University, Utrecht, The Netherlands 2008.

[6] O. V. Dolomanov, L. J. Bourhis, R. J. Gildea, J. A. K. Howard, and H. Puschmann, *J. Appl. Cryst.*, 2009, **42**, 339-341.

[7] L. J. Farrugia, *J. Appl. Cryst.*, 2012, **45**, 849.

[8] POV-Ray Home page, http://www.povray.org/, (accessed March 26, 2018).

[9] M. J. Frisch, G. W. Trucks, H. B. Schlegel, G. E. Scuseria, M. A. Robb, J. R. Cheeseman, G. Scalmani, V. Barone, B. Mennucci, G. A. Petersson, H. Nakatsuji, M. Caricato, X. Li, H. P. Hratchian, A. F. Izmaylov, J. Bloino, G. Zheng, J. L. Sonnenberg, M. Hada, M. Ehara, K. Toyota, R. Fukuda, J. Hasegawa, M. Ishida, T. Nakajima, Y. Honda, O. Kitao, H. Nakai, T. Vreven, J. A. Montgomery, Jr., J. E. Peralta, F. Ogliaro, M. Bearpark, J. J. Heyd, E. Brothers, K. N. Kudin, V. N. Staroverov, R. Kobayashi, J. Normand, K. Radhavachari, A. Rendell, J. C. Burant, S. S. Iyengar, J. Somasi, M. Cossi, N. Rega, N. J. Millam, M. Klene, J. E. Knox, J. B. Cross, V. Bakken, C. Adamo, J. Jaramillo, R. Gomperts, R. E. Stratmann, O. Yazyev, A. J. Austin, R. Cammi, C. Pomelli, J. W. Ochterski, R.

L. Martin, K. Morokuma, V. G. Zakrzewski, G. A. Voth, P. Salvador, J. J. Dannenberg, S. Dapprich, A. D. Daniels, Ö. Farkas, J. B. Foresman, J. V. Ortiz, J. Cioslowski and D. J. Fox, Gaussian 09 (Revision D.01), Gaussian, Inc., Wallingford, CT, 2009.

[10] (a) A. D. Becke, *J. Chem. Phys.*, 1993, **98**, 5648-5652. (b) C. Lee, W. Yang, and R. D. Parr, *Phys. Rev. B*, 1988, **37**, 785-789. (c) P. J. Stephens, F. J. Devlin, C. F. Chabalowski, and M. J. Frisch, *J. Phys. Chem.* 1994, **98**, 11623-11627.